# Joint Power and Bandwidth Allocation in Wireless Cooperative Localization Networks

Tingting Zhang, *Member, IEEE*, Andreas F. Molisch, *Fellow, IEEE*, Yuan Shen, *Member, IEEE*, Qinyu Zhang, *Senior Member, IEEE*, Hao Feng, *Student Member, IEEE*, and Moe Z. Win, *Fellow, IEEE*

***Abstract*— Cooperative localization can enhance the accuracy of wireless network localization by incorporating range information among agent nodes in addition to those between agents and anchors. In this paper, we investigate the optimal allocation of the restricted resources, namely, power and bandwidth, to different nodes. We formulate the optimization problems for both synchronous networks and asynchronous networks, where one way and round trip measurements are applied for range estimation, respectively. Since the optimization problems are nonconvex, we develop an iterative linearization-based technique, and show by comparison with brute-force search that it provides near-optimal performance in the investigated cases. We also show that especially in the case of inefficient anchor placement and/or severe shadowing, cooperation among agents is important and more resources should be allocated to the agents correspondingly.**

***Index Terms*— Cooperative localization, ranging, resource allocation, optimization.**

## I. Introduction

### A. Background and Motivation

POSITION information is the basis of numerous wireless applications and services, such as 911 localization, search and rescue work, asset tracking, vehicle routing, and intruder detection [1]–[6]. For example, position information is of importance in wireless sensor networks for environment monitoring, or firefighers in buildings with fire and heavy smoke. Position estimation is usually accomplished via the Global Positioning System (GPS). However, GPS positions may be inaccurate under certain conditions, such as indoors or in urban environments, since the signals from the GPS satellites suffer from shadowing by obstacles, reflections, etc. An attractive alternative for those situations is wireless network localization with terrestrial reference nodes [7]–[12].

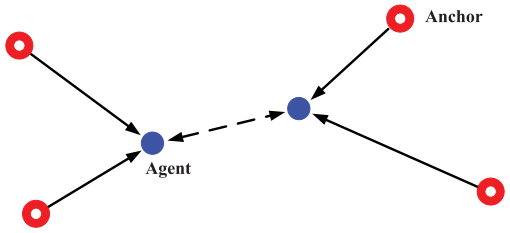


Fig. 1. Cooperative wireless localization network: The agents (blue dot) are located by measurements from both anchors (red circle) and agents.

Location-aware networks generally consist of two kinds of nodes: anchors with known positions and agents with unknown positions (see Fig. 1). The positions of agents are to be determined based on the measurements from multiple nodes.[1] Depending on the positioning technique, the angle of arrival (AOA), the received signal strength (RSS) or time of arrival (TOA) information can be used to determine the location of a node [13], [14].

Conventional wireless localization usually refers to a process in which the positions of agents are determined only by the measurements with respect to the *anchors* only (but not between agents). Localization accuracy in wireless networks is determined by the network topology and the accuracy of the range measurements. Therefore, high-accuracy localization can only be achieved by high-power anchors or high-density anchor deployment, both of which are impractical in cost- and complexity-restricted scenarios (e.g., wireless sensor networks). An appropriate alternative is *cooperative localization*, where agent nodes determine the range between each other and use this information to enhance localization, in particular in those areas that are not covered by sufficient anchors [15]–[17]. In Fig. 1, for example, since each agent is in the transmission range of only two anchors, neither agent

Manuscript received October 3, 2015; revised March 3, 2016; accepted May 27, 2016. This work was supported in part by the Office of Naval Research under Grant N00014-11-1-0397, the National Scientific Foundation of China under Grant 61101124, Grant 91338112, and Grant 61501279, the National Science and Technology Major Project of China under Grant 2013ZX03001022, the National High Technology Research and Development Program ("863" Program) of China under Grant 2014AA01A704, and the Shenzhen Fundamental Research Project uneer Grant JCY2015093015034185. The views expressed in this paper are those of the authors and need not reflect those of ONR. This paper was presented in part at the 2014 IEEE International Conference on Communications. The associate editor coordinating the review of this paper and approving it for publication was H.-C. Wu.

T. Zhang and Q. Zhang are with the Communication Research Center, Shenzhen Graduate School, Harbin Institute of Technology, Shenzhen 518055, China (e-mail: zhangtt@hitsz.edu.cn; zqy@hit.edu.cn).

A. F. Molisch and H. Feng are with the Department of Electronic Engineering, University of Southern California, Los Angeles, CA 90089 USA (e-mail: molisch@usc.edu; haofeng@usc.edu).

Y. Shen was with the Wireless Information and Network Sciences Laboratory, Massachusetts Institute of Technology, Cambridge, MA 02139 USA. He is now with the Tsinghua National Laboratory for Information Science and Technology, Department of Electronic Engineering, Tsinghua University, Beijing 100084, China (e-mail: shenyuan_ee@tsinghua.edu.cn).

M. Z. Win is with the Laboratory for Information and Decision System, Massachusetts Institute of Technology, Cambridge, MA 02139 USA (e-mail: moewin@mit.edu).

Color versions of one or more of the figures in this paper are available online at http://ieeexplore.ieee.org.

Digital Object Identifier 10.1109/TWC.2016.2580504

[1] In centralized networks, the positions of agents can be achieved by a central server, while in the distributed networks, the agents have to perform location inference by themselves.

can trilaterate its position based only on the information from its neighboring anchors. However, cooperation enables both agents to be localized.

Generally, network localization consists of two highly interrelated operations: location inference and resource control. The former performs inference algorithms to determine the positions of agents using range measurements, while the latter performs allocation of the resources for the range measurements [18]. The positions of agents obtained in the former operation provide priori knowledge for the resource allocation, namely power and bandwidth, those are subject to constraints, among the nodes. It is thus important to use those resources in the most efficient way, that determines the accuracy of agents' position estimates.

### B. Related Work

In [19] and [20], the fundamental limits of cooperative wideband localization have been derived in terms of squared position error bound (SPEB) based on the equivalent Fisher information matrix (EFIM). It was shown that the localization accuracy is affected, inter alia, by network topology, propagation channel conditions, signal waveforms, transmit power, etc. Since network topology and channel conditions are usually determined by external circumstances, joint power and bandwidth allocation (JPBA) among wireless nodes (both agents and anchors) is the key tool for resource-restricted system design.

Some work has been carried out on power allocation optimization in localization and radar systems, most of which are non-cooperative scenarios. In [21], a cognitive radar network system for multiple target tracking is proposed. Optimal antenna scheduling and power allocation schemes are discussed. A greedy algorithm is applied for adaptive antenna selection and power optimization, which is similar to the optimal anchor selection problem in non-cooperative localization scenarios. In [22], SPEB is considered as the objective function, by which the power optimization problem is formulated as a semidefinite programming (SDP) problem. In [23], the Cramer-Rao lower bound (CRLB) is used as a performance metric. Two different energy efficient strategies are proposed for target localization. Since the problems are nonconvex, proper approximation methods are proposed. The authors in [24] focus on sparsity of optimal power distribution among anchors. The minimum number of anchors required for single agent localization is thus derived and proved. Some similar work is carried out in distributed multiple radar applications, which can be equivalently regarded as passive localization. Energy efficient and robust power allocation strategies in active localization networks are considered in [25]. On the other hand, rather limited work can be found in the cooperative localization scenario. The authors in [26] also use SDP to solve power allocation problems in RSS-based cooperative localization networks. Low complexity distributed power allocation strategies in cooperative networks are given in [24].

Besides the power allocation, bandwidth allocation is also an important issue for two reasons. First, in pure power allocation strategies, an ideal medium access control (MAC) protocol is required for network design. In [22], each anchor is assumed to perform the transmission over the whole bandwidth. If there are not enough time slots for each transmission (e.g., in most real-time target tracking applications), multiple nodes will have to perform measurements simultaneously. Therefore, appropriate bandwidth allocation strategies to avoid interference are necessary. Second, proper bandwidth allocation also has an important effect on the localization accuracy, especially for the TOA-based ranging and localization techniques. However, to the best of the authors' knowledge, limited work can be found on the bandwidth allocation in localization networks. The only related work is [27], in which the authors focus on power and bandwidth joint optimization in multiple input and multiple output (MIMO) radar systems. This is in contrast to bandwidth optimization in *communications* networks, where considerable work has been done, see [28] and references therein.

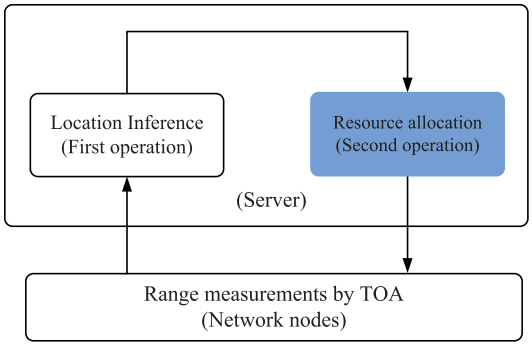


Fig. 2. The architecture of centralized network localization & navigation. The resource allocation part is the main focus of this paper.

Another important issue is that most existing work on resource allocation described above is carried out in synchronous localization networks, which is often impractical for distributed applications. Rather limited work is performed in asynchronous networks, which leads to quite different problem formulations, especially under cooperative conditions.

### C. Main Contributions

As shown in Fig. 2, this paper focuses on the second operation, aiming to optimize the joint power and bandwidth allocation among the resource-restricted nodes in *centralized* TOA-based cooperative localization networks. The main contributions of this paper are as follows.

- We formulate general optimal cooperative JPBA frameworks that exploit the structure of EFIM for both synchronous and asynchronous networks.
- We propose an iterative linearization-based algorithm to solve the nonconvex JPBA problems. This algorithm is computationally efficient and able to find near optimal solutions in the investigated cases. Compared to a pure power allocation strategy, JPBA is superior in both accuracy and energy efficiency.
- We quantify the accuracy performance of various JPBA strategies. Optimal resource allocation solutions among

the network are also studied. Proper cooperation rules (optimal and efficient) can be drawn based on the proposed framework and special constraints.

*Notations:* We use lowercase and uppercase bold symbols to denote vectors and matrices, respectively. The operation tr(**A**) denotes the trace of matrix **A**; the superscripts $(\cdot)^{\mathrm{T}}$ and $||\cdot||$ denote the transpose and Euclidean norm of its argument, $\nabla_{\boldsymbol{\theta}}$ denotes the gradient of $\boldsymbol{\theta}$, respectively. We use calligraphic symbols, e.g., $\mathcal{N}$ to denote sets, and $\bar{x}$ to denote averaging $x$.

## II. System Model

### A. Network Settings

Consider a 2-D location-aware network consisting of $N_{\mathrm{a}}$ agents and $N_{\mathrm{b}}$ anchors with known positions. Agents are able to determine their positions through TOA measurements both with anchors and other cooperative agents. The sets of agents and anchors are represented by $\mathcal{N}_{\mathrm{a}} = \{1, 2, \ldots, N_{\mathrm{a}}\}$ and $\mathcal{N}_{\mathrm{b}} = \{N_{\mathrm{a}}+1, N_{\mathrm{a}}+2, \ldots, N_{\mathrm{a}}+N_{\mathrm{b}}\}$, respectively. The position of node $k$ is denoted by $\mathbf{p}_k = [x_k, y_k]^{\mathrm{T}}$, $k \in \mathcal{N}_{\mathrm{a}} \cup \mathcal{N}_{\mathrm{b}}$. The distance between node $k$ and $j$ is the $\ell$-2 norm of the vector from node $j$ to node $k$

$$d_{kj} = ||\mathbf{p}_k - \mathbf{p}_j|| \tag{1}$$

and the angle from node $k$ to $j$ is given by

$$\phi_{kj} = \arctan\Big(\frac{y_k - y_j}{x_k - x_j}\Big). \tag{2}$$

Accounting for multipath propagation, the received waveform at node $j$ from node $k$ is modeled as

$$r_{kj}(t) = \sum_{l=1}^{L_{kj}} \alpha_{kj}^{(l)} s_k(t - \tau_{kj}^{(l)}) + z_{kj}(t), \quad t \in [0, T_{\mathrm{ob}}) \tag{3}$$

where $s_k(t)$ is the transmit signal from node $k$. Waveform $s_k(t)$ is generated from a known waveform $s(t)$ (occupies the whole bandwidth $W$ with normalized energy), that filtered by the bandwidth $w_k$. Parameters $\alpha_{kj}^{(l)}$ and $\tau_{kj}^{(l)}$ are the amplitude and delay of the $l^{\mathrm{th}}$ path respectively, $L_{kj}$ is the number of multipath components, $z_{kj}(t)$ represents additive white Gaussian noise (AWGN) with two-side power spectral density $N_0/2$, and $[0, T_{\mathrm{ob}})$ is the observation interval.

TOA estimation is applied for range measurements between nodes in this paper. We first consider the synchronous networks (i.e., all agents and anchors work with ideally synchronized clocks) in which one way ranging (OWR) is used for range estimation. Then in Section IV, asynchronous networks are considered, in which round trip TOA measurement is applied.

### B. Position Error Bound

As defined in [20] and [29], the squared position error bound (SPEB) is derived from the equivalent Fisher information matrix (EFIM). The definition of SPEB of agent $k$ is

$$\mathbb{E}\{||\hat{\mathbf{p}}_k - \mathbf{p}_k||^2\} \geq \mathcal{P}(\mathbf{p}_k) \triangleq \mathrm{tr}\{\mathbf{J}_{\mathrm{e}}^{-1}(\mathbf{p}_k)\} \tag{4}$$

where $\mathbf{J}_{\mathrm{e}}(\mathbf{p}_k)$ is the EFIM of agent $k$'s position obtained by measurements, and $\hat{\mathbf{p}}_k$ is an estimate of position $\mathbf{p}_k$.

It has been shown in [20] that the network EFIM of $N_{\mathrm{a}}$ agents in a cooperative localization network can be written as a $2N_{\mathrm{a}} \times 2N_{\mathrm{a}}$ matrix,

$$\mathbf{J}_{\mathrm{e}}^{\mathrm{G}} = \begin{bmatrix} \mathbf{J}_{11} & \cdots & \mathbf{J}_{1N_{\mathrm{a}}} \\ \cdots & \mathbf{J}_{ij} & \cdots \\ \mathbf{J}_{N_{\mathrm{a}}1} & \cdots & \mathbf{J}_{N_{\mathrm{a}}N_{\mathrm{a}}} \end{bmatrix} \tag{5}$$

where

$$\mathbf{J}_{ij} = \begin{cases} \mathbf{J}_{\mathrm{e}}^{\mathrm{A}}(\mathbf{p}_i) + \sum_{k \neq i} \mathbf{C}_{i,k} & i = j \\ -\mathbf{C}_{i,j} & i \neq j. \end{cases} \tag{6}$$

The total SPEB of all agents (termed *global* SPEB in this paper) can thus be obtained as

$$\sum_{k=1}^{N_{\mathrm{a}}} \mathcal{P}(\mathbf{p}_k) \triangleq \mathrm{tr}\{\big(\mathbf{J}_{\mathrm{e}}^{\mathrm{G}}\big)^{-1}\}. \tag{7}$$

In (6), $\mathbf{J}_{\mathrm{e}}^{\mathrm{A}}(\mathbf{p}_k)$ and $\mathbf{C}_{kj}$ are the ranging information (RI) of agent $k$ obtained from all $N_{\mathrm{b}}$ anchors and agent $j$, respectively, expressed as

$$\mathbf{J}_{\mathrm{e}}^{\mathrm{A}}(\mathbf{p}_k) = \sum_{j \in \mathcal{N}_{\mathrm{b}}} \lambda_{kj} \mathbf{q}_{kj} \mathbf{q}_{kj}^{\mathrm{T}} \tag{8}$$

$$\mathbf{C}_{kj} = \mathbf{C}_{jk} = (\lambda_{kj} + \lambda_{jk}) \mathbf{q}_{kj} \mathbf{q}_{kj}^{\mathrm{T}} \tag{9}$$

where $\mathbf{q}_{kj} = [\cos(\phi_{kj}), \sin(\phi_{kj})]^{\mathrm{T}}$, and $\lambda_{kj}$ is termed "range information intensity (RII)", which is defined as the inverse of the bound for squared ranging error [29]. Non-cooperative localization networks can be treated as a special case of cooperative ones with $\mathbf{C}_{ij} = \mathbf{0}$ in (6).

SPEB characterizes the fundamental limit of localization accuracy, and provides valuable performance benchmarks and insights to the system design. Furthermore, SPEB is a tight bound (achievable) in high SNR regimes. So we choose SPEB as the performance metric for location-aware networks in our work.

## III. Optimal JPBA in Synchronous Networks

In this section, we start with the optimal JPBA problem in synchronous cooperative localization networks, where all agents and anchors work with perfectly synchronized clocks.

### A. Range Information Intensity

Based on the definition of SPEB, RII plays an important role in localization accuracy problems. In synchronous networks, range information between node $k$ and $j$ can be obtained by OWR

$$\hat{d}_{kj} = c\,\Delta t \tag{10}$$

where $c$ is the speed of light in free space, and $\Delta t$ is the TOA measurement results.

*Proposition 1:* The RII in synchronous networks using OWR can be represented as

$$\lambda_{kj} = \xi_{kj} \frac{P_k \beta_k^2}{d_{kj}^{\varrho}} \tag{11}$$

where $\xi_{kj}$ is called *ranging channel gain* (RCG) between node $k$ and $j$, $\varrho$ indicates the pathloss coefficient, and $P_k$ and $\beta_k$ are

normalized power and effective bandwidth allocated to node $k$ during measurements.

*Proof:* See the Appendix.

*Remark 1:* We consider the modulated communications systems in this paper, where the carrier phase information is not exploited for TOA estimation [30]. In such a case, the effective bandwidth is equivalent (or proportional) to the real signal bandwidth if the baseband signal waveform is suitably chosen (e.g., sinc-shaped pulses). Nevertheless, when fully coherent reception is applied, the contribution of carrier information is another major factor to be considered for TOA estimation [31].

According to Proposition 1, global SPEB in (7) can be represented as the function of normalized power and bandwidth allocation, which are the main resources to be optimized.

### B. Single Time Slot JPBA Formulation

We first consider only one time slot available for localization in the network, which implies that all measurements have to be performed simultaneously. Global SPEB is considered as the objective function to be minimized. Normalized power and bandwidth allocation solutions among all nodes to be optimized can be represented as $(N_\mathrm{a} + N_\mathrm{b}) \times 1$ vectors,

$$\mathbf{P} = [P_1, P_2, \ldots, P_{N_\mathrm{a}+N_\mathrm{b}}]^\mathrm{T}, \quad \boldsymbol{\beta} = [\beta_1, \beta_2, \ldots, \beta_{N_\mathrm{a}+N_\mathrm{b}}]^\mathrm{T}. \quad (12)$$

The problem can be formulated as

$$\mathscr{P}_\mathrm{S}^1: \ \min. \ \sum_{k\in\mathcal{N}_\mathrm{a}} \mathcal{P}\big(\mathbf{p}_k; \{P_i, \beta_i\}\big) \quad (13)$$

$$\text{s.t.} \quad 0 \le P_i \le P_0 \ \text{ and } \ 0 \le \beta_i \le B_0 \quad (14)$$

$$\sum_{i\in\mathcal{N}_\mathrm{a}\cup\mathcal{N}_\mathrm{b}} P_i \le P_\mathrm{total} \quad (15)$$

$$\sum_{i\in\mathcal{N}_\mathrm{a}\cup\mathcal{N}_\mathrm{b}} \beta_i \le B_\mathrm{total}. \quad (16)$$

Constraint (14) shows that each node has an upper limit on transmission bandwidth $B_0$ and peak power constraint $P_0$ due to the hardware design. Constraint (15) gives the upper bound of total power ($P_\mathrm{total}$). This constraint is derived from the interference point of view, which reflects the amount of overall interference transmitted. Constraint (16) is added to avoid frequency overlaps among different nodes. All nodes are assumed to work on the same carrier frequency, which implies $B_\mathrm{total} = B_0$ in this formulation.

Note that, SPEB is essentially determined by many network parameters which are unknown, such as the positions of agents and channel properties. In this paper, we assume all related parameters are known beforehand. So $\mathscr{P}_\mathrm{S}^1$ and problems formulated later are called "optimal" JPBA problems, by which the performance benchmarks can be obtained. However, in realistic location aware networks, we need to obtain these parameters first. For example, the channel parameters can be obtained by various types of maximum-likelihood estimators [32] or sparse estimation algorithms [33]. Due to the uncertainties of these network parameters, the "robust" JPBA frameworks (based on the "optimal" ones) are thus required to handle this issue in the future. Some related solutions can be found in [31] and [34].

### C. Multiple Time Slots JPBA Formulation

The single time slot framework can be easily extended to the multiple time slots scenario, which is a *static* network scheduling optimization problem. If there are $N_\mathrm{t}$ time slots available, the resource allocation solutions will extend to $(N_\mathrm{a} + N_\mathrm{b}) \times N_\mathrm{t}$ matrices instead of vectors in (12). The set of time slots is represented by $\mathcal{N}_\mathrm{t} = \{1, 2, \ldots, N_\mathrm{t}\}$. Power and bandwidth of node $i$ at time slot $t$ are denoted by $P_{i,t}$ and $\beta_{i,t}$, respectively. Compared to the single slot scenario, the peak and total power constraints are similar, and are rewritten as

$$0 \le P_{i,t} \le P_0 \quad (17)$$

$$\sum_{t=1}^{N_\mathrm{t}} \sum_{i=1}^{N_\mathrm{a}+N_\mathrm{b}} P_{i,t} \le P_\mathrm{total}. \quad (18)$$

Bandwidth allocation is different the single-slot scenario. An extra constraint on total bandwidth available is required, which is $B_\mathrm{total} = N_\mathrm{t} B_0$. In each time slot, the related bandwidth constraints are the same as problem $\mathscr{P}_\mathrm{S}^1$. Bandwidth constraints are summarized as follows

$$0 \le \beta_{i,t} \le B_0 \quad \forall i, t \quad (19)$$

$$\sum_{i=1}^{N_\mathrm{a}+N_\mathrm{b}} \beta_{i,t} \le N_\mathrm{t} B_0 \quad \forall t \quad (20)$$

$$\sum_{t=1}^{N_\mathrm{t}} \sum_{i=1}^{N_\mathrm{a}+N_\mathrm{b}} \beta_{i,t} \le N_\mathrm{t} B_0. \quad (21)$$

Therefore, the problem formulation for multiple time slots is

$$\mathscr{P}_\mathrm{S}^2: \ \min. \ \sum_{k\in\mathcal{N}_\mathrm{a}} \mathcal{P}(\mathbf{p}_k; \{P_{i,t}, \beta_{i,t}\})$$
$$\text{s.t.} \quad (17) - (21).$$

### D. Different JPBA Schemes

To simplify the notation, $P_\mathrm{anchor}$, $B_\mathrm{anchor}$, $P_\mathrm{agent}$ and $B_\mathrm{agent}$ are henceforth used to represent the sum of power and bandwidth resources for anchors and agents, respectively

$$\sum_{t=1}^{N_\mathrm{t}} \sum_{k=1}^{N_\mathrm{a}} P_{k,t} = P_\mathrm{agent}, \sum_{t=1}^{N_\mathrm{t}} \sum_{k=1}^{N_\mathrm{a}} \beta_{k,t} = B_\mathrm{agent}$$
$$\sum_{t=1}^{N_\mathrm{t}} \sum_{j=1}^{N_\mathrm{b}} P_{j,t} = P_\mathrm{anchor}, \sum_{t=1}^{N_\mathrm{t}} \sum_{j=1}^{N_\mathrm{b}} \beta_{j,t} = B_\mathrm{anchor}.$$

The single slot scenario is treated as a special case with $N_\mathrm{t} = 1$. Constraints in $\mathscr{P}_\mathrm{S}^1$ and $\mathscr{P}_\mathrm{S}^2$ can be rewritten as

$$P_\mathrm{anchor} + P_\mathrm{agent} \le P_\mathrm{total} \quad (22)$$

$$B_\mathrm{anchor} + B_\mathrm{agent} \le B_\mathrm{total} \quad (23)$$

$$0 \le P_{k,t} \le P_0, \ 0 \le \beta_{k,t} \le B_0 \quad (24)$$

which is named as a fully flexible (FF) allocation scheme in this paper.

Based on the constraints in the FF scheme, four more allocation schemes may be attained by introducing extra constraints.

- Power flexible scheme (PF). In PF, besides the global constraints (22) - (24), a constraint on the bandwidth allocation on $B_{\text{anchor}}$ and $B_{\text{agent}}$ is given, i.e.,
$$B_{\text{anchor}} = B_{\text{agent}} = \frac{1}{2}B_{\text{total}}. \tag{25}$$
- Bandwidth flexible scheme (BF). Similar to PF, an extra constraint on power allocation is added.
$$P_{\text{anchor}} = P_{\text{agent}} = \frac{1}{2}P_{\text{total}}. \tag{26}$$
- Equally allocation scheme (EA). Both constraints on power and bandwidth (25) - (26) are added.
- Purely uniform allocation scheme (PUA). Each node is allocated the same amount of resources, i.e.,
$$P_i = \frac{1}{N_{\text{a}}+N_{\text{b}}}P_{\text{total}} \quad \text{and} \quad \beta_i = \frac{1}{N_{\text{a}}+N_{\text{b}}}B_{\text{total}}.$$

These schemes give different constraints on the resource allocation for further evaluation. A special case of PF is to set $B_{\text{total}} = 2B_0$. Then measurements by anchors and agents are carried out in two individual time slots, respectively. In EA, it means that the agents' cooperation is regarded to be as important as anchors. Since anchors usually provide higher localization accuracy due to their known positions, the scheme is less efficient. However, the extra constraints make the optimization problem much simpler to solve, as the anchor optimization and agent optimization can be performed separately. PUA is not an optimized resource allocation scheme, and is only used for performance comparison here.

## IV. Optimal JPBA in Asynchronous Networks

The perfect synchronization assumption is often not fulfilled in wireless networks. We thus also consider an asynchronous scenario, where the problem formulation is different. Round trip measurements (RTM) are applied for range estimation where a minimum of two time slots is required.[2] Correspondingly, the network scheduling strategy is firstly described, based on which the resource allocation problems can be formulated.

In the first time slot, measurements are initiated by agents in a broadcast way. After that, in order to fulfill the RTM, anchors and selected *cooperative* agents are allowed to reply in the second time slot (small time stamps are attached for different processing time $\Delta t$ for each agent). Due to the practical half-duplex transceivers, agents are permitted to simultaneously transmit and receive signals only on different frequency bands. Therefore, range information not only between the agent and anchors, but also among different agents can be achieved.

[2]Timing accuracy required for ranging is extremely high (on the order of nanoseconds). However, time slots division (on the millisecond order) can be easily achieved by existing synchronization methods in communications networks. However, they are still treated as asynchronous networks for ranging and localization.

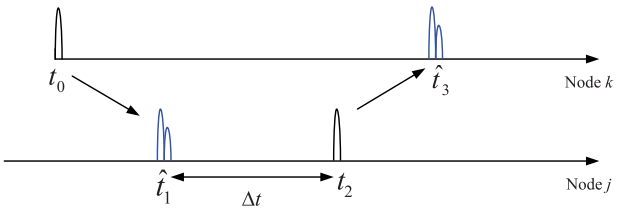


Fig. 3. Range estimation by the round trip measurement of impulse radio signals.

### A. Asynchronous RII

As shown in Fig. 3, in asynchronous networks, range information between node $k$ and $j$ can be obtained by round trip measurements,

$$\hat{d} = \frac{c}{2}[(\hat{t}_3 - t_0) - (t_2 - \hat{t}_1)] \tag{27}$$

where $\hat{t}_3$ and $\hat{t}_1$ are TOA estimation results by node $k$ and $j$. Therefore, the error variance of $\hat{d}$ can be obtained by

$$\sigma_{\text{d}}^2 = \frac{c^2}{4}(\sigma_3^2 + \sigma_1^2) = \frac{1}{4}(\frac{1}{\lambda_{jk}} + \frac{1}{\lambda_{kj}}) \tag{28}$$

where $\lambda_{kj}$ is RII by OWR from node $k$ to node $j$ defined in (11).

Since the measurement on link $k$ to $j$ is symmetric, we have $\xi_{kj} = \xi_{jk}$ and $d_{kj} = d_{jk}$. Asynchronous RII ($\tilde{\lambda}_{kj}$) of RTM in (28) can thus be rewritten as

$$\tilde{\lambda}_{kj} = \frac{1}{\sigma_{\text{d}}^2} = \xi_{kj}\frac{4P_{k,1}\beta_{k,1}^2 P_{j,2}\beta_{j,2}^2}{d_{kj}^{\varrho}(P_{k,1}\beta_{k,1}^2 + P_{j,2}\beta_{j,2}^2)}. \tag{29}$$

### B. Optimal JPBA Formulation in Different Schemes

If there are only the minimally required two time slots available , i.e., $\mathcal{N}_{\text{t}} = \{1, 2\}$, all nodes are generally allowed to transmit signals in both time slots. Similar to the synchronous scenario, the individual and interference constraints still hold in this section, i.e.,

- Individual constraints. Each node has an upper limit on transmission bandwidth $B_0$ and peak power $P_0$.
$$\beta_{i,t} \le B_0 \quad \text{and} \quad P_{i,t} \le P_0, \quad i \in \mathcal{N}_{\text{a}} \cup \mathcal{N}_{\text{b}} \quad t \in \mathcal{N}_{\text{t}}. \tag{30}$$
- Interference constraints. In each time slot, in order to avoid interferences to the receivers, transmission bands from all nodes are not allowed overlap.
$$\sum_{j=1}^{N_{\text{b}}}\beta_{j,1} + \sum_{k=1}^{N_{\text{a}}}\beta_{k,1} \le B_0 \tag{31}$$
$$\sum_{j=1}^{N_{\text{b}}}\beta_{j,2} + \sum_{k=1}^{N_{\text{a}}}\beta_{k,2} \le B_0. \tag{32}$$
- Global power constraints. Two different schemes are considered here. For non-power flexible (NPF) scheme, agents and anchors have their own total power constraints ($P_{\text{agent}}$ and $P_{\text{anchor}}$) respectively. On the other hand, there

is only one total power constraint ($P_{\text{total}}$) in the power flexible (PF) scheme. Therefore, in NPF, the total power constraints should be

$$\sum_{t=1}^{2}\sum_{k=1}^{N_{\text{a}}} P_{k,t} \le P_{\text{agent}} \tag{33}$$

$$\sum_{t=1}^{2}\sum_{j=1}^{N_{\text{b}}} P_{j,t} \le P_{\text{anchor}}. \tag{34}$$

In the PF scheme, the global power constraints should be

$$\sum_{t=1}^{2}\sum_{k=1}^{N_{\text{a}}} P_{k,t} + \sum_{t=1}^{2}\sum_{j=1}^{N_{\text{b}}} P_{j,t} \le P_{\text{total}}. \tag{35}$$

Based on the presented scheduling strategy, the asynchronous optimal JPBA problem modeling can thus be simplified, i.e., agents are allowed to transmit in both time slots, while anchors are only active in the second time slot, i.e.,

$$P_{j,1} = \beta_{j,1} = 0, \quad j \in \mathcal{N}_{\text{b}}. \tag{36}$$

A special case of the non-cooperative localization is realized by setting following constraints

$$P_{j,1} = \beta_{j,1} = 0, \quad j \in \mathcal{N}_{\text{b}} \tag{37}$$

$$P_{k,2} = \beta_{k,2} = 0, \quad k \in \mathcal{N}_{\text{a}}. \tag{38}$$

Global SPEB is still applied as the objective function. The cooperative JPBA problem in PF schemes is formulated as

$$\mathscr{P}_{\text{A}}^{1}: \ \min. \quad \sum_{k\in\mathcal{N}_{\text{a}}} \mathcal{P}(\mathbf{p}_k, \{P_{i,t}, \beta_{i,t}\})$$
$$\text{s.t.} \quad (30)-(32),\ (35),\ (36).$$

The NPF problem $\mathscr{P}_{\text{A}}^{2}$ can be obtained by replacing (35) with (33) and (34) in $\mathscr{P}_{\text{A}}^{1}$. Similarly, the counterparts in the non-cooperative scenario can be further obtained by replacing constraint (36) with (37) and (38) in $\mathscr{P}_{A}^{1}$ and $\mathscr{P}_{\text{A}}^{2}$.

Unfortunately, the JPBA problem with multiple time slots ($N_{\text{t}} > 2$) in asynchronous localization networks is complicated, and essentially NP-hard. Unlike the synchronous scenario, there does not exist a general optimal scheduling strategy. Some preliminary works can be found in [35] and [36]. This problem will be addressed in our future work.

## V. Optimization Algorithms

### A. A Trust Region Framework for Nonconvex Approximation

Although the constraints in all problems above are affine, JPBA optimizations in synchronous and asynchronous networks ($\mathscr{P}_{\text{S}}$ and $\mathscr{P}_{\text{A}}$) are both nonconvex due to the objective functions. We have to depend on techniques designed for nonconvex optimization which do not lead to the global optimal solution in most cases [37]. A reliable and robust framework for nonconvex approximation is called *Trust Region*, by which the original problem is approximated and solved with a sequence of convex problems. The trust region algorithms can even be applied to ill-conditioned problems, and proved to have very strong convergence properties [38]–[40].

The key idea of the trust region framework is that, the approximate model is only "trusted" in a region near the current iterate. For example, at the $m^{\text{th}}$ iteration, the nonconvex function $f(\boldsymbol{\theta})$ is approximated as

$$f(\boldsymbol{\theta}^{(m)}) = \tilde{f}(\boldsymbol{\theta}^{(m)})$$
$$||\boldsymbol{\theta}^{(m)} - \boldsymbol{\theta}^{(m-1)}||_2 \le R^{(m)} \tag{39}$$

where $\tilde{f}(\boldsymbol{\theta})$ is the convex approximation, and $\boldsymbol{\theta}^{(m-1)}$ is the solution obtained in the $m-1^{\text{th}}$ iteration, which is applied as the starting point in the next iteration. Parameter $R^{(m)}$ is the trust region radius at current iteration, which is usually determined by the $\ell$-2 norm.

In trust region algorithms, one important issue is to decide the trust region trial step and whether a trial step should be accepted. The predicted reduction $P_{\text{red}}^{(m)}$ and actual reduction $A_{\text{red}}^{(m)}$ at $m^{\text{th}}$ iteration are defined respectively

$$P_{\text{red}}^{(m)} = |\tilde{f}(\boldsymbol{\theta}^{(m)}) - \tilde{f}(\boldsymbol{\theta}^{(m-1)})|$$
$$A_{\text{red}}^{(m)} = |f(\boldsymbol{\theta}^{(m)}) - f(\boldsymbol{\theta}^{(m-1)})|.$$

The ratio between $P_{\text{red}}^{(m)}$ and $A_{\text{red}}^{(m)}$ is defined as

$$\mu^{(m)} = \frac{P_{\text{red}}^{(m)}}{A_{\text{red}}^{(m)}}. \tag{40}$$

By comparing to a preset threshold, $\mu^{(m)}$ is applied to decide whether the trial step is acceptable and to adjust the new trust region radius. Generally speaking, if $\mu^{(m)}$ indicates that the approximate model fits the original problem well, the trust region can be enlarged. Otherwise, the trust region should be reduced. More details about the trust region frameworks can be found in [38], [40], and references therein.

### B. Taylor Linearization Method

In this section, a Taylor linearization (TL) approximation method based on the trust region framework is presented to solve the asynchronous JPBA problems.[3] Synchronous problems ($\mathscr{P}_{\text{S}}^{1}$ and $\mathscr{P}_{\text{S}}^{2}$) can be treated as special cases and solved accordingly.

In $\mathscr{P}_{\text{A}}^{1}$ and $\mathscr{P}_{\text{A}}^{2}$, only the objective functions are nonconvex due to the asynchronous RII ($\tilde{\lambda}_{kj}$) in (29). According to the trust region framework, we perform Taylor linearization on $\tilde{\lambda}_{kj}$ around a certain expansion point, and then. $\tilde{\lambda}_{kj}$ can be rewritten as (41), shown at the bottom of this page, combined with two trust region constraints

$$||\mathbf{P} - \mathbf{P}^{(m-1)}|| = ||\Delta\mathbf{P}|| \le R_{\mathbf{P}}^{(m)} \tag{42}$$

$$||\boldsymbol{\beta} - \boldsymbol{\beta}^{(m-1)}|| = ||\Delta\boldsymbol{\beta}|| \le R_{\boldsymbol{\beta}}^{(m)}. \tag{43}$$

[3]Here we take the PF scheme for example, while NPF can be treated as a special case of PF.

$$\tilde{\lambda}_{kj}(\mathbf{P}, \boldsymbol{\beta}) \approx \tilde{\lambda}_{kj}^{\text{TL}}(\mathbf{P}, \boldsymbol{\beta}) = \tilde{\lambda}_{kj}(\mathbf{P}^{(m-1)}, \boldsymbol{\beta}^{(m-1)}) + \nabla_{\mathbf{P}}\tilde{\lambda}_{kj}(\mathbf{P}^{(m-1)})\Delta\mathbf{P} + \nabla_{\boldsymbol{\beta}}\tilde{\lambda}_{kj}(\boldsymbol{\beta}^{(m-1)})\Delta\boldsymbol{\beta} \tag{41}$$

**Algorithm 1** A TL-Based Iterative Approximate Algorithm

1: Starting point selection. $\mathbf{P} = \mathbf{P}^{(0)}$, $\boldsymbol{\beta} = \boldsymbol{\beta}^{(0)}$, $m = 0$.
2: **while** convergence not satisfied
3: Solve the problem $\mathscr{P}_{\mathrm{A}}^{3}$. **Output**: $\Delta\mathbf{P}$ and $\Delta\boldsymbol{\beta}$.
4: Solution update: $\mathbf{P}^{(m+1)}$ and $\boldsymbol{\beta}^{(m+1)}$ according to $\mu^{(m)}$.
**if** $\mu^{(m)} < \mu_1$
$\mathbf{P}^{(m+1)} = \mathbf{P}^{(m)}$, $\boldsymbol{\beta}^{(m+1)} = \boldsymbol{\beta}^{(m)}$
**else**
$\mathbf{P}^{(m+1)} = \mathbf{P}^{(m)} + \Delta\mathbf{P}$, $\boldsymbol{\beta}^{(m+1)} = \boldsymbol{\beta}^{(m)} + \Delta\boldsymbol{\beta}$
**end**
5: Trust region radius update.
**if** $\mu^{(m)} < \mu_1$
$R_{\mathbf{P}}^{(m+1)} = c_1||\Delta\mathbf{P}||$, $R_{\boldsymbol{\beta}}^{(m+1)} = c_1||\Delta\boldsymbol{\beta}||$
**else if** $\mu^{(m)} > \mu_2$
$R_{\mathbf{P}}^{(m+1)} = \min\{c_2 R_{P}^{(m)}, R_{P}^{\star}\}$,
$R_{\boldsymbol{\beta}}^{(m+1)} = \min\{c_2 R_{\beta}^{(m)}, R_{\beta}^{\star}\}$
**else**
$R_{\mathbf{P}}^{(m+1)} = ||\Delta\mathbf{P}||$, $R_{\boldsymbol{\beta}}^{(m+1)} = ||\Delta\boldsymbol{\beta}||$
**end**
6: Convergence checking. $m = m + 1$.
7: **end**
8: **Output**: Optimal $\mathbf{P}$ and $\boldsymbol{\beta}$, Minimized SPEB.

By inserting $\tilde{\lambda}_{kj}^{\mathrm{TL}}$ into (8) and (9), an approximate SPEB ($\mathcal{P}^{\mathrm{TL}}(\mathbf{p}_k, \{\Delta\mathbf{P}, \Delta\boldsymbol{\beta}\})$) under Taylor linearization is attained.

Regarding the PF-JPBA problem $\mathscr{P}_{\mathrm{A}}^{1}$, an alternative form by Taylor linearization is

$$\mathscr{P}_{\mathrm{A}}^{3}: \ \min. \quad \sum_{k\in\mathcal{N}_{\mathrm{a}}} \mathcal{P}^{\mathrm{TL}}(\mathbf{p}_k, \{\Delta\mathbf{P}, \Delta\boldsymbol{\beta}\})$$
$$\text{s.t.} \quad (30)-(32),\ (35)-(36),\ (42)-(43).$$

*Proposition 2:* Problem $\mathscr{P}_{\mathrm{A}}^{3}$ is convex in $\Delta\mathbf{P}$ and $\Delta\boldsymbol{\beta}$.

*Proof*: The constraints in $\mathscr{P}_{\mathrm{A}}^{3}$ are affine, only the convexity of objective function is required here. Based on the rules of convex analysis, the convexity is closed under composition with an affine mapping [37]. Since the function $\mathrm{tr}\{\mathbf{X}^{-1}\}$ is convex when $\mathbf{X} \succ 0$, and RII ($\tilde{\lambda}_{kj}^{\mathrm{TL}}(\mathbf{P}, \boldsymbol{\beta})$) is joint affine in $\Delta\mathbf{P}$ and $\Delta\boldsymbol{\beta}$ after Taylor linearization, problem $\mathscr{P}_{\mathrm{A}}^{3}$ thus is proved convex.

According to the trust region framework, the trust radius and solutions are updated in an adaptive way based on the predictive quality ($\mu^{(m)}$) after $m^{\mathrm{th}}$ iteration.

- If the approximate model ($\mathcal{P}^{\mathrm{TL}}$) predicts the actual improvement well, or if there is even more improvement, we increase the radius $R^{(m)}$ and allow a longer step at the next iteration.
- If the model does a bad job in predicting, we decrease the size of the trust region in the next iteration, and recalculate $\Delta\theta$. Repeat this iteration step with the updated smaller trust region.
- Finally, if the model does an acceptable job of predicting the improvement in $\mathcal{P}$, we keep the size of the trust region.

An iterative approximation algorithm based on Taylor linearization is given in Algorithm 1. Since the JPBA problems are essentially nonconvex, only local convergence can be guaranteed. Therefore, we can run the approximation algorithm from multiple initial points and take the best result as the final solution [41]. At step 1 of Algorithm 1, two different starting points are thus considered in Algorithm 1.

1) Starting point 1 provides uniform allocation to the anchor nodes, while not providing any power to the agent nodes.
2) Starting point 2 provides an equal amount of resources to all anchor and agent nodes.

We choose positive constants $\mu_1 < \mu_2 < 1$ and $c_1 < 1$, $c_2 > 1$. Usually $\mu_1$ is small positive to keep any computed "good" points. Typically values for $\mu_1$ and $\mu_2$ are $\mu_1 = 0.10$ and $\mu_2 = 0.75$ [39]. $R_{\mathbf{P}}^{\star}$ and $R_{\boldsymbol{\beta}}^{\star}$ are the preset trust radius upper bounds of power and bandwidth, respectively.

In step 6, if the relative difference between SPEB achieved in the previous and current steps is small enough (compared to a preset threshold $\epsilon$), the iteration ends.

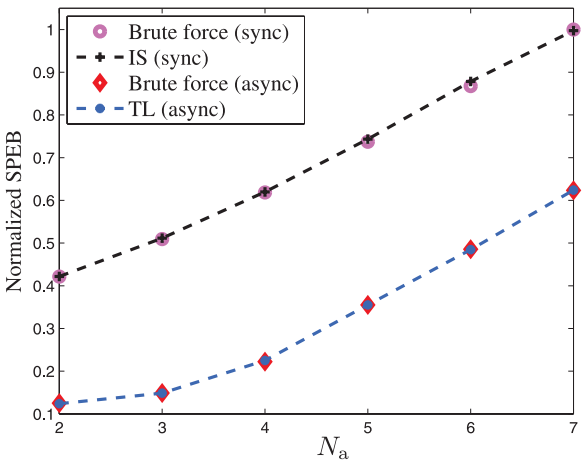


Fig. 4. Results comparison to the brute force search.

### C. Accuracy Evaluations of TL

Since the optimal JPBA problems are essentially nonconvex, the accuracy of the approximate algorithm is evaluated by comparisons to a (time consuming) brute force search. We first perform uniform JPBA among anchors. Optimal JPBA among agents are then achieved by TL and brute force respectively. Note that the solution might be inferior to the solution of the FF scheme; we present this example here purely to evaluate the accuracy of our solution methods.

Note that the global optimum *cannot be guaranteed by TL*. But it can be seen from Fig. 4 that, the accuracy achieved by TL is close to the brute force method. On the other hand, TL is much more computationally efficient, which makes it an appropriate option to optimal JPBA problems in both synchronous and asynchronous localization networks.

## VI. Numerical Results

### A. Network Settings

In this section, we present numerical examples for the localization performance based on the proposed JPBA schemes. A typical ranging scenario using impulse radio UWB signals (CM1 in IEEE 802.15.4a channel model [42]) is considered to

TABLE I
TYPICAL PARAMETERS IN UWB RANGING

| $W$ | $\nu$ | $\bar{\gamma}_{\mathrm{DP}}$ | $\bar{\chi}_{k_{ij}}$ | Power spectral density | $N_0$ |
|---|---|---|---|---|---|
| 500 (MHz) | 0.1 (m) | 0.2 | 0.32 | -41.3 (dBm/MHz) | -174 (dBm/Hz) |

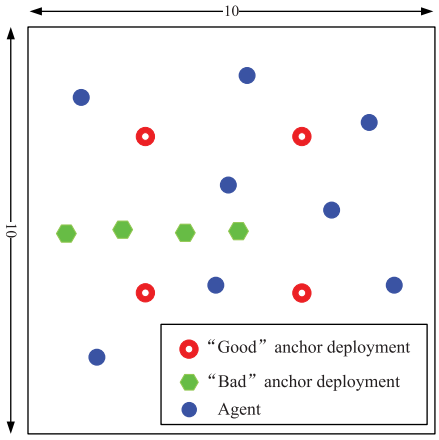


Fig. 5. The location-aware network consisting four anchors and multiple agents, where anchors are deployed in two different ways.

make the results more intuitive. A 2ns duration Gaussian pulse occupying 3.1-3.6GHz spectrum is used as the transmit waveform. The amplitude fading $\varphi_k$ is normalized here. An average RCG between two nodes can be obtained based on the practical parameters in Table I as $\bar{\xi} \approx 152.3$dB by (11). After that, global power ($P_{\mathrm{total}}$) and bandwidth ($B_{\mathrm{total}}$) constraints are normalized. Peak power and bandwidth constraints on each node are $P_0 = 0.4$, $B_0 = 1$ respectively. The path loss and shadowing are considered as the channel gains. Path loss coefficient is set as $\varrho = 2$. TL approach is applied to solve the JPBA problems, in which the two starting points described in Section V-B are investigated. The SPEB convergence rule is applied and the threshold for checking is $\epsilon = 10^{-3}$. The trust region upper bound is set as 0.5 for both $R^{\star}_{\mathbf{P}}$ and $R^{\star}_{\boldsymbol{\beta}}$. $\mu_1 = 0.10$ and $\mu_2 = 0.75$, $c_1 = 0.5$, $c_2 = 1.5$. In synchronous networks, both single and multiple time slots scenarios are considered, while only the two time slot scenario is evaluated in asynchronous networks, as discussed before.

A dense network example is shown in Fig. 5. There are $N_{\mathrm{b}} = 4$ prelocated anchors and $N_{\mathrm{a}}$ agents distributed in a square region, i.e., $U([0, 10] \times [0, 10])$. Adding agents increases the node density. It is widely recognized (see, e.g., [30]) that a good anchor deployment (AP) is on the vertices of a convex hull of the agent positions, to minimize errors. However, note that practical constraints may prevent such a placement. Thus, investigating the effect of AP on global accuracy and agents cooperation is important. For this purpose, we henceforth investigate two different APs shown in Fig. 5, and simply called "good" and "bad" AP.

### B. Synchronous Networks

*1) Single Time Slot Scenario:* We first consider the synchronous scenario with "good" AP in Fig .5. All five cooperative JPBA schemes proposed in Section III-D are implemented and evaluated for their accuracy. It can be seen that

- Total errors of all schemes increase with the number of agents. The main reason for that is the constraints on total power and bandwidth. Similar results are drawn in the non-cooperative scenario with optimal power allocation schemes [22].
- As we predicted in Section III, PUA is the simplest but least efficient scheme, since there is no optimization among resources.
- Compared among the four schemes other than PUA, FF performs best while EA is the worst. This is intuitive, since under constraint for the total resources, more flexibility offers better performance. The power and bandwidth resources can be automatically concentrated in the most helpful nodes, especially when there are no external constraints on it.
- We furthermore observe that BF outperforms PF. The reason is that EFIMs are affected by the square of the bandwidth, $P_j \beta_j^2$, and so bandwidth plays a more important role for the overall accuracy. Another reason is that, there exists an additional peak power constraint ($P_0 < P_{\mathrm{total}}$), which makes the PF scheme actually not completely flexible for power allocation.

Note that the errors shown here, which are in the sub-millimeter range, might not be easy to achieve in practice (similar to [43]). They are predicated on the ideal assumption that full channel state information is obtained, perfect sampling and quantization processing is attained, etc. Evaluations with practical algorithms using measured channel impulse responses (e.g., [44]) show errors that can be orders of magnitude larger. Nevertheless, the optimization frameworks in this paper still hold. Meaningful performance benchmarks and optimal cooperation strategies are provided thereby.

The gain obtained from agents' cooperation is another important issue. In Fig. 6(a), it is obvious that cooperation among agents is able to improve the accuracy in all schemes, but by different amounts. Cooperation is of great help to the performance in PF, when $B_{\mathrm{anchor}}$ is tightly restricted. On the other hand, cooperation gain in FF is quite limited. It means that, when anchors are properly deployed, the performance of non-cooperative localization in FF is close to the optimal solutions, while there is much a larger space for improvement for PF.

In the second scenario, cooperative JPBA solutions with shadowing and bad AP are studied. We use here a simplified shadowing model such that the SNR will decrease by 10 dB in case of a blockage between transmitter and receiver; the probability for such a blockage is $P_{\mathrm{shadowing}} = 0.5$. Due to the space restrictions, only FF is considered here. As shown in Fig. 6(b), it is observed that, when anchors are poorly deployed, cooperation plays a much more important role than in "good" AP scenarios, which agrees well with intuition. It is also obvious that "bad" AP leads to much larger localization errors; yet cooperation among agents will be able to mitigate the error effectively. Similarly, shadowing is an important factor that affects the performance. When anchors are severely blocked, they provide degraded ranging information to the

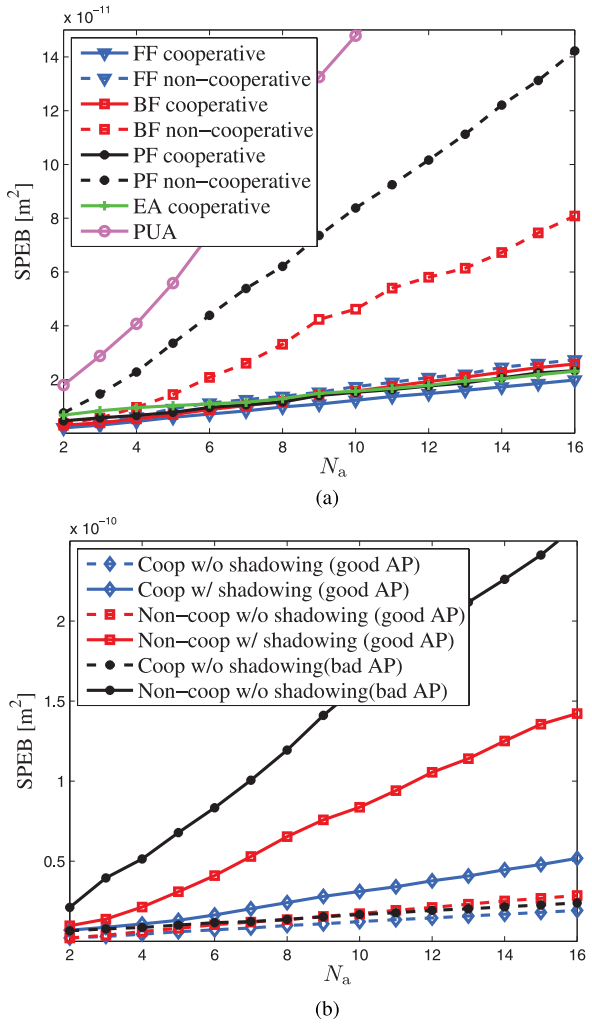


Fig. 6. SPEB results in single-time-slot synchronous networks. (a) Different schemes (in good AP) w/o shadowing. (b) Different channel conditions and APs.

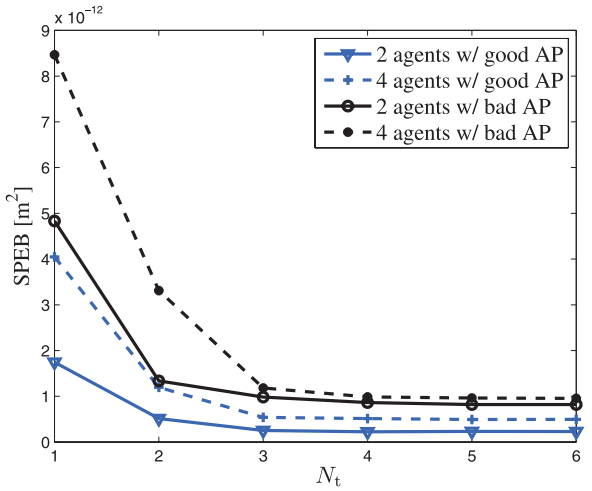


Fig. 7. SPEB results in multiple-time-slot synchronous networks.

agents and hence agent's cooperation plays a more important role in localization.

*2) Multiple Time Slots Scenario:* In this part, FF-JPBA with multiple time slots available are studied, where two and four agents are considered for localization performance evaluation. As shown in Fig. 7, accuracy becomes better with more time

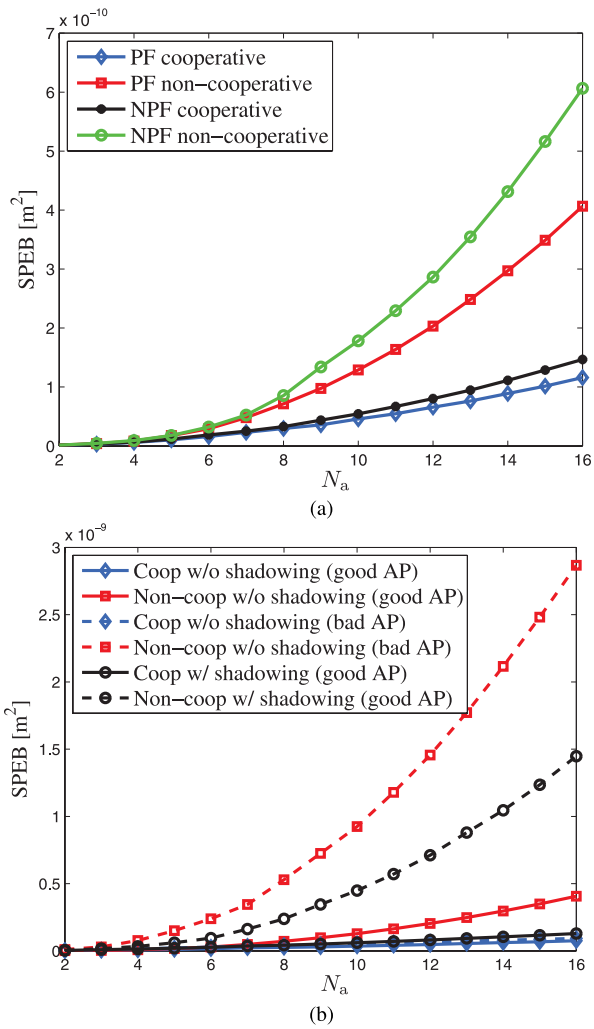


Fig. 8. SPEB results in asynchronous networks. (a) Different schemes (in good AP) w/o shadowing. (b) Different channel conditions and APs.

slots, which agrees with the previous analysis. However, when the number of time slots is more than 3, it shows that the accuracy remains at a certain level. The reason is that, although there are still lot of bandwidth resources available, power resources for measurements have been used up. It is equivalent to the pure power allocation strategy when $N_t$ is large enough for each node to perform individual measurements.

### *C. Asynchronous Networks*

In this section, the accuracy solutions in asynchronous networks with different schemes are studied. Both PF and NPF schemes are evaluated in Fig. 8(a). Shadowing effects and different APs are considered in Fig. 8(b). From the numerical results, it can be concluded that,

- Similar to the synchronous scenario, the total localization error increases with respect to the agent number.
- PF outperforms NPF in accuracy. Similar to the conclusions drawn in the synchronous scenario, more flexibility in resource allocation offers better performance.
- Channel and anchor deployment are still important factors on localization accuracy. When the anchor deployment or the channel condition is poor, cooperation among agents plays a much more important role than under ordinary conditions.

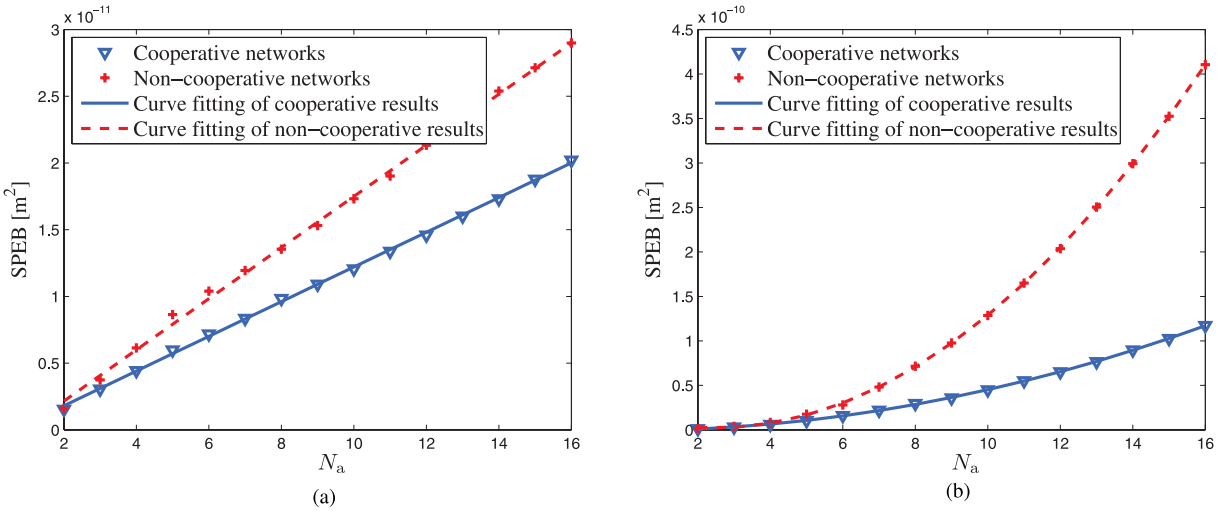


Fig. 9. Scaling analysis of synchronous and asynchronous networks. (a) Synchronous networks. (b) Asynchronous networks.

### *D. Discussions on Accuracy and Scaling Laws*

In this part, we first compare the accuracy between synchronous ($N_t = 1$) and asynchronous ($N_t = 2$) networks. It can be seen from Fig. 9, even though there are two time slots available in the asynchronous localization network (i.e. $B_{\text{total}} = 2B_0$), accuracy performance in the synchronous scenario is much better.

Scaling laws for accuracy show the benefit of cooperation and synchronization in large networks. In Fig. 9, we perform least square (LS) curve fitting over the achieved results in both synchronous and asynchronous networks. It can be seen from Fig. 9(a), global SPEB scales proportional to the number of agents in synchronous networks ($\Theta(N_a)$), which implies the average SPEB in synchronous networks remains nearly constant when a new agent is added. The main reason is that, since we use a broadcast strategy, anchors play the main role in synchronous localization networks (which is also described in detail later in Section VI-E). New agents can generally localize themselves by the broadcasted signals from anchors without extra resources.

On the other hand, SPEB increases quadratically with respect to the number of agents, i.e., $\Theta(N_a^2)$ in Fig. 9(b). It implies that the average SPEB scales as $\Theta(N_a)$ in asynchronous networks. According to the localization strategies in Section IV, all agents and anchors are required to transmit signals. Therefore, if new agents are added, the average resources allocated to each agent decreases proportionally, which leads to a SPEB increase along with the agent number.

Note that our analysis is based on a typical *dense* network. If the measurement is carried out in an *extended* network (network area increases proportional to the number of nodes), the scaling rules are quite different since the pathloss and therefore SNR changes.

### *E. Resource Allocation Solutions*

To analyze the resource allocation solutions, we first consider the optimal allocation ratio between anchors and agents. An auxiliary parameter is defined as

$$\zeta = \frac{P_{\text{anchor}} B_{\text{anchor}}^2}{P_{\text{anchor}} B_{\text{anchor}}^2 + P_{\text{agent}} B_{\text{agent}}^2} \tag{44}$$

which indicates the percentage of resources that are allocated to anchors.

Resource allocation solutions are different in synchronous and asynchronous networks due to the two ranging methods applied. As shown in Fig. 10, agents are kept quiet in synchronous non-cooperative measurements. All resources are used by the anchors, which leads to $\zeta = 1$. Fig. 10(a) shows different resource allocation solutions in synchronous networks. It suggests that when anchors are properly deployed and channel conditions are good, non-cooperative localization achieves close-to-optimum solutions. This conclusion also can be drawn from the FF solutions in Fig. 6(a) and Fig. 6(b). Therefore, most resources are recommended to be allocated to anchors. On the other hand, if anchors are poorly located and channel conditions are not so good, agents' cooperation will be increasingly important as the agents' number increases. Nevertheless, $\zeta$ is still suggested to be greater than 0.5. This agrees with the conclusions in [20] that anchors play the main role during localization in most cases. Another phenomenon is that, since there exists a peak power constraint $P_0 = 0.4$, $\zeta$ in PF is smaller than FF and BF.

In asynchronous networks, agents are required to perform transmission during each RTM, even if in a non-cooperative manner. Therefore, $\zeta$ will thus be much smaller than in the synchronous case. In Fig. 10(b), $\zeta \leq 0.5$ in most non-cooperative cases when $N_a > 3$. A special case of asynchronous JPBA is non-cooperative NPF, where

$$P_{\text{anchor}} = P_{\text{agent}} = 0.5, \quad B_{\text{anchor}} = B_{\text{agent}} = 1$$

and the corresponding $\zeta$ is 0.5. When cooperation among agents is carried out, $\zeta$ is nearly 0.2 smaller than the corresponding non-cooperative $\zeta$. When the agent number is relative large, $\zeta$ is even smaller than 0.1. It implies that, in optimal cooperative asynchronous networks, most of the

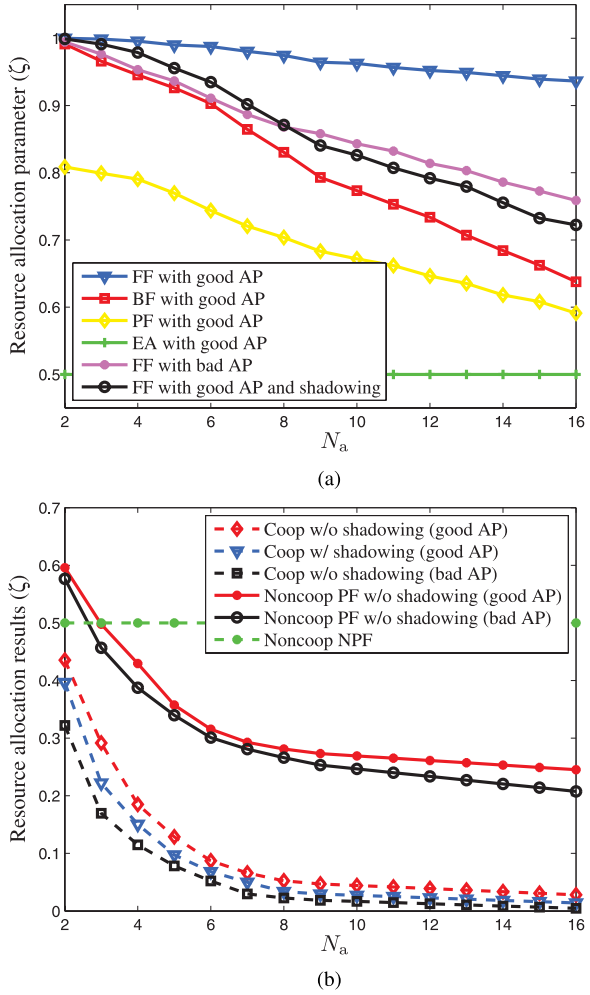


Fig. 10. Resource allocation solutions in different schemes. (a) Sync networks. (b) Async networks.

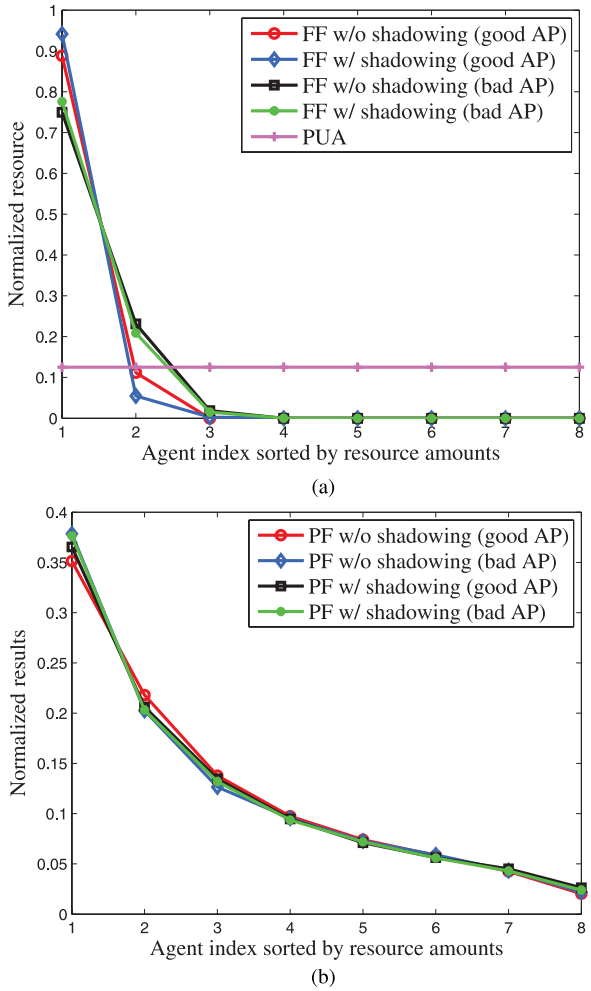


Fig. 11. Resource allocation solutions among cooperative agents. (a) Sync networks. (b) Async networks.

resources are allocated to the agents, which is different from the results drawn from the synchronous scenario.

Optimal resource distribution among agents is helpful to explain how the cooperation among agents works. Fig. 11 shows the resource allocation solutions among eight agents as an example. From Fig. 11(a), in contrast to PUA, all optimized JPBA schemes allocate the resources to the one or two most helpful agents, even in bad AP and shadowing conditions. In other words, the resource distribution among agents is extremely sparse, which is consistent with the power allocation solutions in [24].

However, the distribution of resources is different in the asynchronous networks. In Fig. 11(b), the resource allocation solutions are much more balanced than in Fig. 11(a). One main reason is that, agents must perform transmission during the RTM in both non-cooperative and cooperative localization. A uniform resource allocation strategy may be more suitable in asynchronous localization networks accordingly.

### *F. Moving-Agent Scenarios*

In this part, we consider another typical scenario in GPS-challenged environments. As shown in Fig. 12(a), five agents enter the square area from the left side as a group. Four anchors are prelocated at the vertices of the area. Both synchronous and asynchronous measurements are considered. Optimal JPBA is performed with the movement of the group. SPEB is obtained with respect to the position of the central agent. From the results in Fig. 12(b), some conclusions can be drawn.

- Localization accuracy with synchronization achieved is much better than that in the asynchronous network, which agrees with the results in Fig. 9. In the synchronous system, SPEB achieved by cooperative methods are only slightly better than the non-cooperative ones (e.g., results on $z = -1$ and $z = 11$, etc). But in asynchronous networks, cooperation among agents is able to promote the accuracy obviously in all investigated cases.
- Since the network topology is symmetric during the agents' movement, the solutions obtained are symmetric as well. When the agent group is far away from the anchor area, RII will be relatively small due to the pathloss, which leads to a large localization error.
- When the right two agents (1 and 2) approach the borderline (i.e., $z = -1$), anchor 1 and 2 are nearly on the same line with agents. This is problematic for localization due to the geometric deployment. Therefore, EFIM for localization is mainly provided by anchor 3 and 4, which are far away from the agent group. It leads to a SPEB

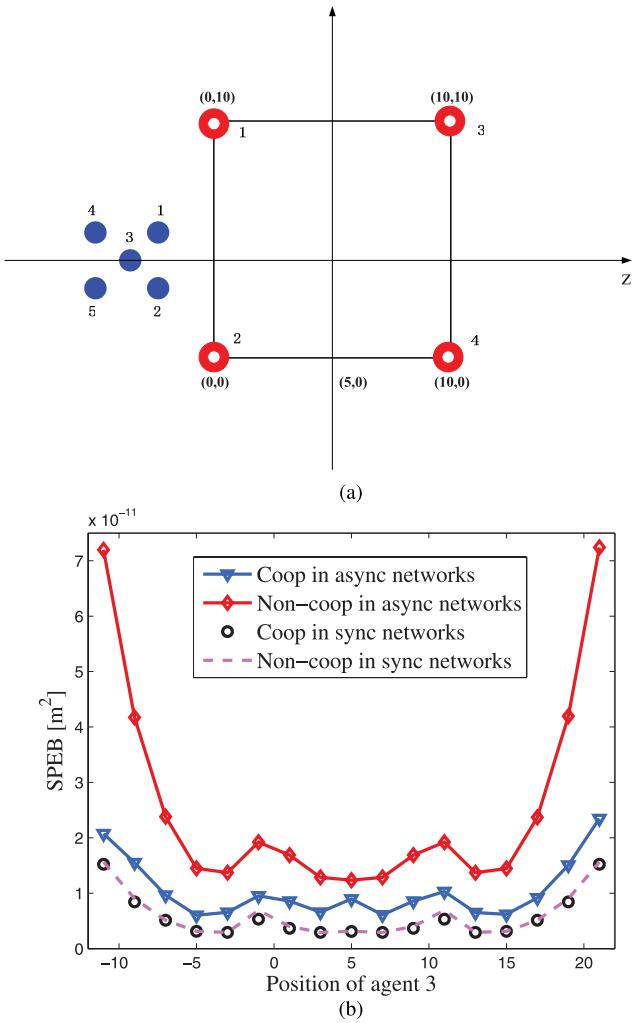


Fig. 12. Accuracy results in moving agents scenario. (a) Moving agents network. (b) Accuracy results with respect to the positions of agents.

peak at $z = -1$. The reason for another SPEB peak at $z = 11$ is similar.

## VII. Conclusion

In this paper, we formulated the optimization problems for resource allocation in cooperative localization systems, where both one-way and two-way ranging are considered. Since the optimization problems are nonconvex, we developed iterative linearization methods that provide efficient numerical solutions, and achieve near-optimal performances in the investigated case studies of simulations. From the simulation results, we can have the following important observations: (i) both bandwidth and power allocation among the nodes are important for good localization performance, where the former is more critical; (ii) cooperation among agents is especially important when anchor placement is bad, and/or severe shadowing occurs, (iii) the optimal resource allocation for one-way ranging is sparse, and (iv) for two-way ranging, the optimal resource allocation is more balanced. These algorithms developed in this paper and the insights obtained from the simulation results can facilitate the design and operation of efficient wireless localization networks.

## Appendix
## Proof of Proposition 1

In [29], the RII between node $k$ and $j$ is defined as

$$\lambda_{kj} = \frac{8\pi^2\tilde{\beta}_k^2}{c^2}(1-\chi_{kj})\mathrm{SNR}_j^{(1)} \tag{45}$$

where $\chi_{kj} \in (0,1)$ is the path-overlap coefficient (POC) that characterizes the effect of multipath propagation for localization, $\tilde{\beta}_k$ is the real effective bandwidth of the transmitted waveform from node $k$, defined as

$$\tilde{\beta}_k = \Big(\frac{\int_{-\infty}^{\infty} f^2|S_k(f)|^2 df}{\int_{-\infty}^{\infty}|S_k(f)|^2 df}\Big)^{1/2} \tag{46}$$

in which $S_k(f)$ is the spectrum of $s_k(t)$. In this paper, we assume that full channel parameters are known beforehand. So the amplitude fading $\varphi_k$ on $s_k(t)$ is known thereafter. Furthermore, $\mathrm{SNR}_j^{(l)}$ is the energy ratio between the $l^{\text{th}}$ multipath component and the noise at node $j$, i.e.,

$$\mathrm{SNR}_j^{(l)} \triangleq \frac{E_l}{N_0} = \frac{\tilde{P}_k|\alpha_j^{(l)}|^2\int_0^{T_{\text{ob}}}|s_k(t)|^2 dt}{N_0} \tag{47}$$

where $\tilde{P}_k$ is the reference transmit power of node $k$ (measured at a reference distance, such as 1 meter away from the transmitter [45]). Since the energy of $s(t)$ is normalized, the energy of the transmitted waveform $s_k(t)$ can be represented as $\varphi_k^2$.

To simplify the notations, we define normalized power and effective bandwidth allocated to node $k$ as $P_k = \tilde{P}_k/P_{\text{peak}}$ and $\beta_k = \tilde{\beta}_k/W$, respectively. Here $P_{\text{peak}}$ and $W$ are peak values of power and effective bandwidth available on each node. We thus have the power of direct path (DP) component as

$$\tilde{P}_k|\alpha_j^{(1)}|^2\varphi_k^2 = \gamma_{\text{DP}}\varphi_k^2 P_{\text{peak}}P_k$$

where $\gamma_{\text{DP}}$ is the ratio of DP power among all multipath components. RII $\lambda_{kj}$ can be rewritten as

$$\begin{aligned}\lambda_{kj} &= \frac{8\pi^2W^2(1-\chi_{kj})\gamma_{\text{DP}}\varphi_k^2P_{\text{peak}}}{c^2N_0}\Big(\frac{\nu}{4\pi\, d_{\text{ref}}}\Big)^2\Big(\frac{d_{\text{ref}}}{d_{kj}}\Big)^{\varrho}P_k\beta_k^2 \\ &= \xi_{kj}\frac{P_k\beta_k^2}{d_{kj}^{\varrho}}\end{aligned} \tag{48}$$

where $\nu$ is the wave length of the transmitted signals. The proof is thus complete.

## References

[1] M. Z. Win *et al.*, "Network localization and navigation via cooperation," *IEEE Commun. Mag.*, vol. 49, no. 5, pp. 56–62, May 2011.

[2] A. H. Sayed, A. Tarighat, and N. Khajehnouri, "Network-based wireless location: Challenges faced in developing techniques for accurate wireless location information," *IEEE Signal Process. Mag.*, vol. 22, no. 4, pp. 24–40, Jul. 2005.

[3] K. Pahlavan, X. Li, and J.-P. Mäkelä, "Indoor geolocation science and technology," *IEEE Commun. Mag.*, vol. 40, no. 2, pp. 112–118, Feb. 2002.

[4] S. Gezici *et al.*, "Localization via ultra-wideband radios: A look at positioning aspects for future sensor networks," *IEEE Signal Process. Mag.*, vol. 22, no. 4, pp. 70–84, Jul. 2005.

[5] D. Jourdan, D. Dardari, and M. Win, "Position error bound for UWB localization in dense cluttered environments," *IEEE Trans. Aerosp. Electron. Syst.*, vol. 44, no. 2, pp. 613–628, Apr. 2008.

[6] R. Niu and P. K. Varshney, "Target location estimation in sensor networks with quantized data," *IEEE Trans. Signal Process.*, vol. 54, no. 12, pp. 4519–4528, Dec. 2006.

[7] Y. Shen, S. Mazuelas, and M. Z. Win, "Network navigation: Theory and interpretation," *IEEE J. Sel. Areas Commun.*, vol. 30, no. 9, pp. 1823–1834, Oct. 2012.

[8] N. Patwari, J. N. Ash, S. Kyperountas, A. O. Hero, R. L. Moses, and N. S. Correal, "Locating the nodes: Cooperative localization in wireless sensor networks," *IEEE Signal Process. Mag.*, vol. 22, no. 4, pp. 54–69, Jul. 2005.

[9] H. Wymeersch, S. Maranò, W. M. Gifford, and M. Z. Win, "A machine learning approach to ranging error mitigation for UWB localization," *IEEE Trans. Commun.*, vol. 60, no. 6, pp. 1719–1728, Jun. 2012.

[10] S. Gezici and H. V. Poor, "Position estimation via ultra-wide-band signals," *Proc. IEEE*, vol. 97, no. 2, pp. 386–403, Feb. 2009.

[11] J. Rantakokko *et al.*, "Accurate and reliable soldier and first responder indoor positioning: Multisensor systems and cooperative localization," *IEEE Wireless Commun.*, vol. 18, no. 2, pp. 10–18, Apr. 2011.

[12] X. Shen and P. K. Varshney, "Sensor selection based on generalized information gain for target tracking in large sensor networks," *IEEE Trans. Signal Process.*, vol. 62, no. 2, pp. 363–375, Jan. 2014.

[13] J. J. Caffery, Jr., *Wireless Location in CDMA Cellular Radio Systems*. New York, NY, USA: Springer Science & Business Media, 2000.

[14] T. Zhang, Q. Zhang, H. Xu, H. Zhang, and B. Zhou, "Research and implementation of a practical ranging method using IR-UWB signals," *IEICE Trans. Commun.*, vol. E96-B, pp. 1976–1985, Jul. 2013.

[15] D. Dardari, A. Conti, J. Lien, and M. Z. Win, "The effect of cooperation on localization systems using UWB experimental data," *EURASIP J. Appl. Signal Process.*, vol. 2008, Feb. 2008, Art. no. 513873.

[16] H. Wymeersch, J. Lien, and M. Z. Win, "Cooperative localization in wireless networks," *Proc. IEEE*, vol. 97, no. 2, pp. 427–450, Feb. 2009.

[17] S. Li, M. Hedley, and I. B. Collings, "New efficient indoor cooperative localization algorithm with empirical ranging error model," *IEEE J. Sel. Areas Commun.*, vol. 33, no. 7, pp. 1407–1417, Jul. 2015.

[18] W. Dai, Y. Shen, and M. Z. Win, "Energy-efficient network navigation algorithms," *IEEE J. Sel. Areas Commun.*, vol. 33, no. 7, pp. 1418–1430, Jul. 2015.

[19] Y. Qi, H. Kobayashi, and H. Suda, "Analysis of wireless geolocation in a non-line-of-sight environment," *IEEE Trans. Wireless Commun.*, vol. 5, no. 3, pp. 672–681, Mar. 2006.

[20] Y. Shen, H. Wymeersch, and M. Z. Win, "Fundamental limits of wideband localization—Part II: Cooperative networks," *IEEE Trans. Inf. Theory*, vol. 56, no. 10, pp. 4981–5000, Oct. 2010.

[21] P. Chavali and A. Nehorai, "Scheduling and power allocation in a cognitive radar network for multiple-target tracking," *IEEE Trans. Signal Process.*, vol. 60, no. 2, pp. 715–729, Feb. 2012.

[22] W. W.-L. Li, Y. Shen, Y. J. Zhang, and M. Z. Win, "Robust power allocation for energy-efficient location-aware networks," *IEEE/ACM Trans. Netw.*, vol. 21, no. 6, pp. 1918–1930, Dec. 2013.

[23] H. Godrich, A. P. Petropulu, and H. V. Poor, "Power allocation strategies for target localization in distributed multiple-radar architectures," *IEEE Trans. Signal Process.*, vol. 59, no. 7, pp. 3226–3240, Jul. 2011.

[24] W. Dai, Y. Shen, and M. Z. Win, "Distributed power allocation for cooperative wireless network localization," *IEEE J. Sel. Areas Commun.*, vol. 33, no. 1, pp. 28–40, Jan. 2015.

[25] T. Wang, G. Leus, and L. Huang, "Ranging energy optimization for robust sensor positioning based on semidefinite programming," *IEEE Trans. Signal Process.*, vol. 57, no. 12, pp. 4777–4787, Dec. 2009.

[26] R. M. Vaghefi, M. R. Gholami, R. M. Buehrer, and E. G. Ström, "Cooperative received signal strength-based sensor localization with unknown transmit powers," *IEEE Trans. Signal Process.*, vol. 61, no. 6, pp. 1389–1403, Mar. 2013.

[27] N. Garcia, A. M. Haimovich, M. Coulon, and M. Lops, "Resource allocation in MIMO radar with multiple targets for non-coherent localization," *IEEE Trans. Signal Process.*, vol. 62, no. 10, pp. 2656–2666, May 2014.

[28] R. Rashtchi, R. H. Gohary, and H. Yanikomeroglu, "Joint routing, scheduling and power allocation in OFDMA wireless ad hoc networks," in *Proc. Int. Conf. Commun.*, Ottawa, ON, Canada, Jun. 2012, pp. 5483–5487.

[29] Y. Shen and M. Z. Win, "Fundamental limits of wideband localization—Part I: A general framework," *IEEE Trans. Inf. Theory*, vol. 56, no. 10, pp. 4956–4980, Oct. 2010.

[30] H. Godrich, A. M. Haimovich, and R. S. Blum, "Target localization accuracy gain in MIMO radar-based systems," *IEEE Trans. Inf. Theory*, vol. 56, no. 6, pp. 2783–2803, Jun. 2010.

[31] T. Zhang, C. Qin, A. F. Molisch, and Q. Zhang, "Joint power and spectrum allocation in wireless localization networks," *IEEE Trans. Commun.*, doi: 10.1109/TCOMM.2016.2580149.

[32] K. Haneda, A. Richter, and A. F. Molisch, "Modeling the frequency dependence of ultra-wideband spatio-temporal indoor radio channels," *IEEE Trans. Antennas Propag.*, vol. 60, no. 6, pp. 2940–2950, Jun. 2012.

[33] N. Michelusi, U. Mitra, A. F. Molisch, and M. Zorzi, "UWB sparse/diffuse channels, part I: Channel models and Bayesian estimators," *IEEE Trans. Signal Process.*, vol. 60, no. 10, pp. 5307–5319, Oct. 2012.

[34] Y. Shen, W. Dai, and M. Z. Win, "Power optimization for network localization," *IEEE/ACM Trans. Netw.*, vol. 22, no. 4, pp. 1337–1350, Aug. 2014.

[35] S. Dwivedi, A. De Angelis, and P. Händel, "Scheduled UWB pulse transmissions for cooperative localization," in *Proc. Int. Conf. Ultra-Wideband*, Syracuse, NY, USA, Sep. 2012, pp. 6–10.

[36] L. Song, T. Zhang, X. Yu, C. Qin, and Q. Zhang, "Scheduling in cooperative UWB localization networks using round trip measurements," *IEEE Commun. Lett.*, vol. 20, no. 7, doi: 10.1109/LCOMM.2016.2558499.

[37] S. Boyd and L. Vandenberghe, *Convex Optimization*. Cambridge, U.K.: Cambridge Univ. Press, 2004.

[38] D. C. Sorensen, "Newton's method with a model trust region modification," *SIAM J. Numer. Anal.*, vol. 19, pp. 409–426, Feb. 1982.

[39] N. M. Alexandrov, J. E. Dennis, Jr., R. M. Lewis, and V. Torczon, "A trust-region framework for managing the use of approximation models in optimization," *Struct. Optim.*, vol. 15, pp. 16–23, Feb. 1998.

[40] Y.-X. Yuan, "A review of trust region algorithms for optimization," in *Proc. Int. Congr. Ind. Appl. Math. (ICIAM)*, vol. 99. 2000, pp. 271–282.

[41] S. Boyd, *Sequential Convex Programming*. Stanford, CA, USA: Stanford Univ. Press, 2008.

[42] A. F. Molisch *et al.*, *IEEE 802.15.4a Channel Model—Final Report*, IEEE Standard P802-15-04, pp. 1–41, 2004.

[43] D. Dardari, A. Conti, U. Ferner, A. Giorgetti, and M. Z. Win, "Ranging with ultrawide bandwidth signals in multipath environments," *Proc. IEEE*, vol. 97, no. 2, pp. 404–426, Feb. 2009.

[44] V. Kristem, A. F. Molisch, S. Niranjayan, and S. Sangodoyin, "Coherent UWB ranging in the presence of multiuser interference," *IEEE Trans. Wireless Commun.*, vol. 13, no. 8, pp. 4424–4439, Aug. 2014.

[45] A. F. Molisch, *Wireless Communications*. New York, NY, USA: Wiley, 2010.

**Tingting Zhang** (M'12) received the B.S. (Hons.) and Ph.D. degrees in electronics engineering from the Harbin Institute of Technology (HIT), Harbin, China, in 2003 and 2009, respectively. From 2009 to 2012, he was a Post-Doctoral Research Fellow with the Communication Engineering Research Center, Shenzhen Graduate School, HIT, Shenzhen, China. From 2012 to 2014, he was with the Department of Electronic Engineering, University of Southern California, Los Angeles, CA, USA, as a Visiting Scholar. He is currently an Associate Professor with the Shenzhen Graduate School, HIT. His main research interests include cooperative localization, ultrawideband technology, and resource allocation. He serves as a TPC Member for several international conferences, such as GLOBECOM, ICCC, and VTC. He is also a Reviewer of numerous academic journals, such as the IEEE JOURNAL ON SELECTED AREAS IN COMMUNICATIONS, the IEEE TRANSACTIONS ON WIRELESS COMMUNICATIONS, and the IEEE TRANSACTIONS ON VEHICULAR TECHNOLOGY. He received the Outstanding Postdoctoral Award of HIT, Shenzhen Graduate School, in 2011. He also received the Shenzhen High Level Talent Program Award in 2012.

**Andreas F. Molisch** (S'89–M'95–SM'00–F'05) received the Dipl.-Ing., Ph.D., and Habilitation degrees from the Technical University of Vienna, Vienna, Austria, in 1990, 1994, and 1999, respectively. He subsequently was with AT&T (Bell) Laboratories Research (USA), Lund University, Lund, Sweden, and Mitsubishi Electric Research Labs (USA). He is currently a Professor of Electrical Engineering and the Director of the Communication Sciences Institute with the University of Southern California, Los Angeles. His current research interests are the measurement and modeling of mobile radio channels, ultrawideband communications and localization, cooperative communications, multiple-input multiple-output systems, wireless systems for healthcare, and novel cellular architectures. He has authored, co-authored, or edited four books [among them the textbook entitled *Wireless Communications* (Wiley-IEEE Press)], 18 book chapters, some 180 journal papers, 260 conference papers, and more than 80 patents and 70 standards contributions. Dr. Molisch has been an Editor of a number of journals and special issues, a General Chair, a Technical Program Committee Chair, or a Symposium Chair of multiple international conferences, and the Chairman of various international standardization groups. He is a Fellow of the National Academy of Inventors, AAAS, and IET, an IEEE Distinguished Lecturer, and a Member of the Austrian Academy of Sciences. He has received numerous awards, among them the Donald Fink Prize of the IEEE, and the Eric Sumner Award of the IEEE.

**Yuan Shen** (S'05–M'14) received the Ph.D. degree and the S.M. degree in electrical engineering and computer science from the Massachusetts Institute of Technology (MIT), Cambridge, MA, USA, in 2014 and 2008, respectively, and the B.E. degree (with highest honor) in electronic engineering from Tsinghua University, Beijing, China, in 2005.

He is an Associate Professor with the Department of Electronic Engineering at Tsinghua University. Prior to joining Tsinghua University, he was a Research Assistant and then Postdoctoral Associate with the Laboratory for Information and Decision Systems (LIDS) at MIT in 2005-2014. His research interests include statistical inference, network science, communication theory, information theory, and optimization. His current research focuses on network localization and navigation, inference techniques, resource allocation, and intrinsic wireless secrecy.

Dr. Shen was a recipient of the Qiu Shi Outstanding Young Scholar Award (2015), the China's Youth 1000-Talent Program (2014), the Marconi Society Paul Baran Young Scholar Award (2010), the MIT EECS Ernst A. Guillemin Best S. M. Thesis Award (1st place) (2008), the Qualcomm Roberto Padovani Scholarship (2008), and the MIT Walter A. Rosenblith Presidential Fellowship (2005). His papers received the IEEE Communications Society Fred W. Ellersick Prize (2012) and three Best Paper Awards from the IEEE Globecom (2011), the IEEE ICUWB (2011), and the IEEE WCNC (2007). He is elected Secretary (2015-2017) for the Radio Communications Committee of the IEEE Communications Society. He serves as symposium Co-Chair of the Technical Program Committee (TPC) for the IEEE Globecom (2016), the European Signal Processing Conference (EUSIPCO) (2016), and the IEEE ICC Advanced Network Localization and Navigation (ANLN) Workshop (2016). He also serves as Editor for the IEEE COMMUNICATIONS LETTERS since 2015 and Guest-Editor for the *International Journal of Distributed Sensor Networks* (2015).

**Qinyu Zhang** (M'08–SM'12) received the bachelor's degree in communication engineering from the Harbin Institute of Technology (HIT) in 1994, and the Ph.D. degree in biomedical and electrical engineering from the University of Tokushima, Japan, in 2003. From 1999 to 2003, he was an Assistant Professor with the University of Tokushima. From 2003 to 2005, he was an Associate Professor with the Shenzhen Graduate School, HIT, and the Founding Director of the Communication Engineering Research Center with the School of Electronic and Information Engineering. Since 2005, he has been a Full Professor, and serves as the Dean of the EIE School. His research interests include aerospace communications and networks, wireless communications and networks, cognitive radios, signal processing,and biomedical engineering.

He is on the Editorial Board of some academic journals, such as the *Journal on Communications*, *KSII Transactions on Internet and Information Systems*, and *Science China: Information Sciences*. He was the TPC Co-Chair of the IEEE/CIC ICCC'15, the Symposium Co-Chair of the IEEE VTC'16 Spring, an Associate Chair for Finance of ICMMT'12, and the Symposium Co-Chair of CHINACOM'11. He has been a TPC Member for INFOCOM, ICC, GLOBECOM, WCNC, and other flagship conferences in communications. He was the Founding Chair of the IEEE Communications Society Shenzhen Chapter.

He has received the National Science Fund for Distinguished Young Scholars, the Young and Middle-Aged Leading Scientist of China, and the Chinese New Century Excellent Talents in University, and obtained three scientific and technological awards from governments.

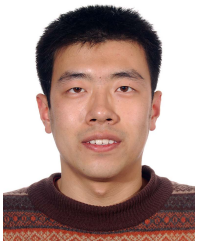

**Hao Feng** received the B.S. degree from the Department of Information Science and Electronic Engineering (ISEE), Zhejiang University, Hangzhou, China, in 2006, and the M.S. degree from the Wireless Communication Laboratory, ISEE, Zhejiang University, in 2008. He is currently pursuing the Ph.D. degree with the Department of Electrical Engineering, University of Southern California, Los Angeles, CA, USA. He has been with the Wireless Devices and Systems Group. He is a recipient of the Annenberg Graduate Fellowship for his Ph.D. study. His research interests include stochastic network optimization, cross-layer optimization, and cooperative communications with their applications in cloud networks, wireless ad-hoc networks, and wireless localization networks.

**Moe Z. Win** (S'85–M'87–SM'97–F'04) received both the Ph.D. in Electrical Engineering and the M.S. in Applied Mathematics as a Presidential Fellow at the University of Southern California (USC) in 1998. He received the M.S. in Electrical Engineering from USC in 1989 and the B.S. (*magna cum laude*) in Electrical Engineering from Texas A&M University in 1987.

He is a Professor at the Massachusetts Institute of Technology (MIT) and the founding director of the Wireless Information and Network Sciences Laboratory. Prior to joining MIT, he was with AT&T Research Laboratories for five years and with the Jet Propulsion Laboratory for seven years. His research encompasses fundamental theories, algorithm design, and experimentation for a broad range of real-world problems. His current research topics include network localization and navigation, network interference exploitation, intrinsic wireless secrecy, adaptive diversity techniques, and ultra-wideband systems.

Professor Win is an elected Fellow of the AAAS, the IEEE, and the IET, and was an IEEE Distinguished Lecturer. He was honored with two IEEE Technical Field Awards: the IEEE Kiyo Tomiyasu Award (2011) and the IEEE Eric E. Sumner Award (2006, jointly with R. A. Scholtz). Together with students and colleagues, his papers have received numerous awards, including the IEEE Communications Society's Stephen O. Rice Prize, (2012) the IEEE Aerospace and Electronic Systems Society's M. Barry Carlton Award (2011), the IEEE Communications Society's Guglielmo Marconi Prize Paper Award (2008), and the IEEE Antennas and Propagation Society's Sergei A. Schelkunoff Transactions Prize Paper Award (2003).

Dr. Win was an elected Member-at-Large on the IEEE Communications Society Board of Governors (2011-2013). He was the Chair (2004-2006) and Secretary (2002-2004) for the Radio Communications Committee of the IEEE Communications Society. Over the last decade, he has organized and chaired numerous international conferences.

# Joint Power and Bandwidth Allocation in Wireless Cooperative Localization Networks

Tingting Zhang, *Member, IEEE*, Andreas F. Molisch, *Fellow, IEEE*, Yuan Shen, *Member, IEEE*, Qinyu Zhang, *Senior Member, IEEE*, Hao Feng, *Student Member, IEEE*, and Moe Z. Win, *Fellow, IEEE*

***Abstract*— Cooperative localization can enhance the accuracy of wireless network localization by incorporating range information among agent nodes in addition to those between agents and anchors. In this paper, we investigate the optimal allocation of the restricted resources, namely, power and bandwidth, to different nodes. We formulate the optimization problems for both synchronous networks and asynchronous networks, where one way and round trip measurements are applied for range estimation, respectively. Since the optimization problems are nonconvex, we develop an iterative linearization-based technique, and show by comparison with brute-force search that it provides near-optimal performance in the investigated cases. We also show that especially in the case of inefficient anchor placement and/or severe shadowing, cooperation among agents is important and more resources should be allocated to the agents correspondingly.**

***Index Terms*— Cooperative localization, ranging, resource allocation, optimization.**

## I. Introduction

### A. Background and Motivation

POSITION information is the basis of numerous wireless applications and services, such as 911 localization, search and rescue work, asset tracking, vehicle routing, and intruder detection [1]–[6]. For example, position information is of importance in wireless sensor networks for environment monitoring, or firefighers in buildings with fire and heavy smoke. Position estimation is usually accomplished via the Global Positioning System (GPS). However, GPS positions may be inaccurate under certain conditions, such as indoors or in urban environments, since the signals from the GPS satellites suffer from shadowing by obstacles, reflections, etc. An attractive alternative for those situations is wireless network localization with terrestrial reference nodes [7]–[12].

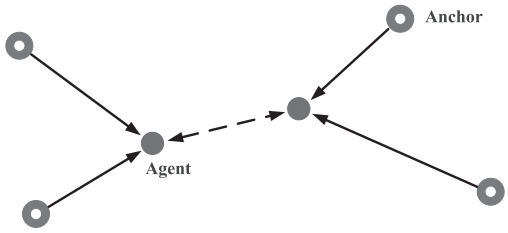


Fig. 1. Cooperative wireless localization network: The agents (blue dot) are located by measurements from both anchors (red circle) and agents.

Location-aware networks generally consist of two kinds of nodes: anchors with known positions and agents with unknown positions (see Fig. 1). The positions of agents are to be determined based on the measurements from multiple nodes.[1] Depending on the positioning technique, the angle of arrival (AOA), the received signal strength (RSS) or time of arrival (TOA) information can be used to determine the location of a node [13], [14].

Conventional wireless localization usually refers to a process in which the positions of agents are determined only by the measurements with respect to the *anchors* only (but not between agents). Localization accuracy in wireless networks is determined by the network topology and the accuracy of the range measurements. Therefore, high-accuracy localization can only be achieved by high-power anchors or high-density anchor deployment, both of which are impractical in cost- and complexity-restricted scenarios (e.g., wireless sensor networks). An appropriate alternative is *cooperative localization*, where agent nodes determine the range between each other and use this information to enhance localization, in particular in those areas that are not covered by sufficient anchors [15]–[17]. In Fig. 1, for example, since each agent is in the transmission range of only two anchors, neither agent

Manuscript received October 3, 2015; revised March 3, 2016; accepted May 27, 2016. This work was supported in part by the Office of Naval Research under Grant N00014-11-1-0397, the National Scientific Foundation of China under Grant 61101124, Grant 91338112, and Grant 61501279, the National Science and Technology Major Project of China under Grant 2013ZX03001022, the National High Technology Research and Development Program ("863" Program) of China under Grant 2014AA01A704, and the Shenzhen Fundamental Research Project uneer Grant JCY2015093015034185. The views expressed in this paper are those of the authors and need not reflect those of ONR. This paper was presented in part at the 2014 IEEE International Conference on Communications. The associate editor coordinating the review of this paper and approving it for publication was H.-C. Wu.

T. Zhang and Q. Zhang are with the Communication Research Center, Shenzhen Graduate School, Harbin Institute of Technology, Shenzhen 518055, China (e-mail: zhangtt@hitsz.edu.cn; zqy@hit.edu.cn).

A. F. Molisch and H. Feng are with the Department of Electronic Engineering, University of Southern California, Los Angeles, CA 90089 USA (e-mail: molisch@usc.edu; haofeng@usc.edu).

Y. Shen was with the Wireless Information and Network Sciences Laboratory, Massachusetts Institute of Technology, Cambridge, MA 02139 USA. He is now with the Tsinghua National Laboratory for Information Science and Technology, Department of Electronic Engineering, Tsinghua University, Beijing 100084, China (e-mail: shenyuan_ee@tsinghua.edu.cn).

M. Z. Win is with the Laboratory for Information and Decision System, Massachusetts Institute of Technology, Cambridge, MA 02139 USA (e-mail: moewin@mit.edu).

Color versions of one or more of the figures in this paper are available online at http://ieeexplore.ieee.org.

Digital Object Identifier 10.1109/TWC.2016.2580504

[1] In centralized networks, the positions of agents can be achieved by a central server, while in the distributed networks, the agents have to perform location inference by themselves.

can trilaterate its position based only on the information from its neighboring anchors. However, cooperation enables both agents to be localized.

Generally, network localization consists of two highly interrelated operations: location inference and resource control. The former performs inference algorithms to determine the positions of agents using range measurements, while the latter performs allocation of the resources for the range measurements [18]. The positions of agents obtained in the former operation provide priori knowledge for the resource allocation, namely power and bandwidth, those are subject to constraints, among the nodes. It is thus important to use those resources in the most efficient way, that determines the accuracy of agents' position estimates.

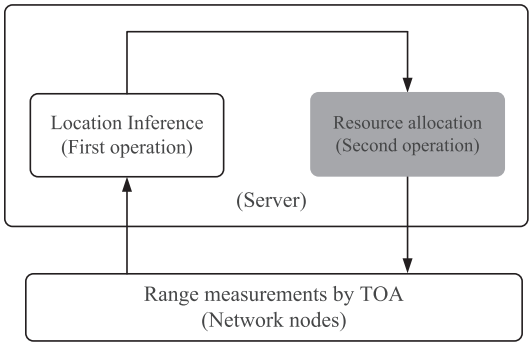


Fig. 2. The architecture of centralized network localization & navigation. The resource allocation part is the main focus of this paper.

### B. Related Work

In [19] and [20], the fundamental limits of cooperative wideband localization have been derived in terms of squared position error bound (SPEB) based on the equivalent Fisher information matrix (EFIM). It was shown that the localization accuracy is affected, inter alia, by network topology, propagation channel conditions, signal waveforms, transmit power, etc. Since network topology and channel conditions are usually determined by external circumstances, joint power and bandwidth allocation (JPBA) among wireless nodes (both agents and anchors) is the key tool for resource-restricted system design.

Some work has been carried out on power allocation optimization in localization and radar systems, most of which are non-cooperative scenarios. In [21], a cognitive radar network system for multiple target tracking is proposed. Optimal antenna scheduling and power allocation schemes are discussed. A greedy algorithm is applied for adaptive antenna selection and power optimization, which is similar to the optimal anchor selection problem in non-cooperative localization scenarios. In [22], SPEB is considered as the objective function, by which the power optimization problem is formulated as a semidefinite programming (SDP) problem. In [23], the Cramer-Rao lower bound (CRLB) is used as a performance metric. Two different energy efficient strategies are proposed for target localization. Since the problems are nonconvex, proper approximation methods are proposed. The authors in [24] focus on sparsity of optimal power distribution among anchors. The minimum number of anchors required for single agent localization is thus derived and proved. Some similar work is carried out in distributed multiple radar applications, which can be equivalently regarded as passive localization. Energy efficient and robust power allocation strategies in active localization networks are considered in [25]. On the other hand, rather limited work can be found in the cooperative localization scenario. The authors in [26] also use SDP to solve power allocation problems in RSS-based cooperative localization networks. Low complexity distributed power allocation strategies in cooperative networks are given in [24].

Besides the power allocation, bandwidth allocation is also an important issue for two reasons. First, in pure power allocation strategies, an ideal medium access control (MAC) protocol is required for network design. In [22], each anchor is assumed to perform the transmission over the whole bandwidth. If there are not enough time slots for each transmission (e.g., in most real-time target tracking applications), multiple nodes will have to perform measurements simultaneously. Therefore, appropriate bandwidth allocation strategies to avoid interference are necessary. Second, proper bandwidth allocation also has an important effect on the localization accuracy, especially for the TOA-based ranging and localization techniques. However, to the best of the authors' knowledge, limited work can be found on the bandwidth allocation in localization networks. The only related work is [27], in which the authors focus on power and bandwidth joint optimization in multiple input and multiple output (MIMO) radar systems. This is in contrast to bandwidth optimization in *communications* networks, where considerable work has been done, see [28] and references therein.

Another important issue is that most existing work on resource allocation described above is carried out in synchronous localization networks, which is often impractical for distributed applications. Rather limited work is performed in asynchronous networks, which leads to quite different problem formulations, especially under cooperative conditions.

### C. Main Contributions

As shown in Fig. 2, this paper focuses on the second operation, aiming to optimize the joint power and bandwidth allocation among the resource-restricted nodes in *centralized* TOA-based cooperative localization networks. The main contributions of this paper are as follows.

- We formulate general optimal cooperative JPBA frameworks that exploit the structure of EFIM for both synchronous and asynchronous networks.
- We propose an iterative linearization-based algorithm to solve the nonconvex JPBA problems. This algorithm is computationally efficient and able to find near optimal solutions in the investigated cases. Compared to a pure power allocation strategy, JPBA is superior in both accuracy and energy efficiency.
- We quantify the accuracy performance of various JPBA strategies. Optimal resource allocation solutions among

the network are also studied. Proper cooperation rules (optimal and efficient) can be drawn based on the proposed framework and special constraints.

*Notations:* We use lowercase and uppercase bold symbols to denote vectors and matrices, respectively. The operation tr(**A**) denotes the trace of matrix **A**; the superscripts $(\cdot)^{\mathrm{T}}$ and $||\cdot||$ denote the transpose and Euclidean norm of its argument, $\nabla_{\boldsymbol{\theta}}$ denotes the gradient of $\boldsymbol{\theta}$, respectively. We use calligraphic symbols, e.g., $\mathcal{N}$ to denote sets, and $\bar{x}$ to denote averaging $x$.

## II. System Model

### A. Network Settings

Consider a 2-D location-aware network consisting of $N_{\mathrm{a}}$ agents and $N_{\mathrm{b}}$ anchors with known positions. Agents are able to determine their positions through TOA measurements both with anchors and other cooperative agents. The sets of agents and anchors are represented by $\mathcal{N}_{\mathrm{a}} = \{1, 2, \ldots, N_{\mathrm{a}}\}$ and $\mathcal{N}_{\mathrm{b}} = \{N_{\mathrm{a}}+1, N_{\mathrm{a}}+2, \ldots, N_{\mathrm{a}}+N_{\mathrm{b}}\}$, respectively. The position of node $k$ is denoted by $\mathbf{p}_k = [x_k, y_k]^{\mathrm{T}}$, $k \in \mathcal{N}_{\mathrm{a}} \cup \mathcal{N}_{\mathrm{b}}$. The distance between node $k$ and $j$ is the $\ell$-2 norm of the vector from node $j$ to node $k$

$$d_{kj} = ||\mathbf{p}_k - \mathbf{p}_j|| \tag{1}$$

and the angle from node $k$ to $j$ is given by

$$\phi_{kj} = \arctan\Big(\frac{y_k - y_j}{x_k - x_j}\Big). \tag{2}$$

Accounting for multipath propagation, the received waveform at node $j$ from node $k$ is modeled as

$$r_{kj}(t) = \sum_{l=1}^{L_{kj}} \alpha_{kj}^{(l)} s_k(t - \tau_{kj}^{(l)}) + z_{kj}(t), \quad t \in [0, T_{\mathrm{ob}}) \tag{3}$$

where $s_k(t)$ is the transmit signal from node $k$. Waveform $s_k(t)$ is generated from a known waveform $s(t)$ (occupies the whole bandwidth $W$ with normalized energy), that filtered by the bandwidth $w_k$. Parameters $\alpha_{kj}^{(l)}$ and $\tau_{kj}^{(l)}$ are the amplitude and delay of the $l^{\mathrm{th}}$ path respectively, $L_{kj}$ is the number of multipath components, $z_{kj}(t)$ represents additive white Gaussian noise (AWGN) with two-side power spectral density $N_0/2$, and $[0, T_{\mathrm{ob}})$ is the observation interval.

TOA estimation is applied for range measurements between nodes in this paper. We first consider the synchronous networks (i.e., all agents and anchors work with ideally synchronized clocks) in which one way ranging (OWR) is used for range estimation. Then in Section IV, asynchronous networks are considered, in which round trip TOA measurement is applied.

### B. Position Error Bound

As defined in [20] and [29], the squared position error bound (SPEB) is derived from the equivalent Fisher information matrix (EFIM). The definition of SPEB of agent $k$ is

$$\mathbb{E}\{||\hat{\mathbf{p}}_k - \mathbf{p}_k||^2\} \geq \mathcal{P}(\mathbf{p}_k) \triangleq \mathrm{tr}\{\mathbf{J}_{\mathrm{e}}^{-1}(\mathbf{p}_k)\} \tag{4}$$

where $\mathbf{J}_{\mathrm{e}}(\mathbf{p}_k)$ is the EFIM of agent $k$'s position obtained by measurements, and $\hat{\mathbf{p}}_k$ is an estimate of position $\mathbf{p}_k$.

It has been shown in [20] that the network EFIM of $N_{\mathrm{a}}$ agents in a cooperative localization network can be written as a $2N_{\mathrm{a}} \times 2N_{\mathrm{a}}$ matrix,

$$\mathbf{J}_{\mathrm{e}}^{\mathrm{G}} = \begin{bmatrix} \mathbf{J}_{11} & \cdots & \mathbf{J}_{1N_{\mathrm{a}}} \\ \cdots & \mathbf{J}_{ij} & \cdots \\ \mathbf{J}_{N_{\mathrm{a}}1} & \cdots & \mathbf{J}_{N_{\mathrm{a}}N_{\mathrm{a}}} \end{bmatrix} \tag{5}$$

where

$$\mathbf{J}_{ij} = \begin{cases} \mathbf{J}_{\mathrm{e}}^{\mathrm{A}}(\mathbf{p}_i) + \sum_{k \neq i} \mathbf{C}_{i,k} & i = j \\ -\mathbf{C}_{i,j} & i \neq j. \end{cases} \tag{6}$$

The total SPEB of all agents (termed *global* SPEB in this paper) can thus be obtained as

$$\sum_{k=1}^{N_{\mathrm{a}}} \mathcal{P}(\mathbf{p}_k) \triangleq \mathrm{tr}\{\big(\mathbf{J}_{\mathrm{e}}^{\mathrm{G}}\big)^{-1}\}. \tag{7}$$

In (6), $\mathbf{J}_{\mathrm{e}}^{\mathrm{A}}(\mathbf{p}_k)$ and $\mathbf{C}_{kj}$ are the ranging information (RI) of agent $k$ obtained from all $N_{\mathrm{b}}$ anchors and agent $j$, respectively, expressed as

$$\mathbf{J}_{\mathrm{e}}^{\mathrm{A}}(\mathbf{p}_k) = \sum_{j \in \mathcal{N}_{\mathrm{b}}} \lambda_{kj} \mathbf{q}_{kj} \mathbf{q}_{kj}^{\mathrm{T}} \tag{8}$$

$$\mathbf{C}_{kj} = \mathbf{C}_{jk} = (\lambda_{kj} + \lambda_{jk}) \mathbf{q}_{kj} \mathbf{q}_{kj}^{\mathrm{T}} \tag{9}$$

where $\mathbf{q}_{kj} = [\cos(\phi_{kj}), \sin(\phi_{kj})]^{\mathrm{T}}$, and $\lambda_{kj}$ is termed "range information intensity (RII)", which is defined as the inverse of the bound for squared ranging error [29]. Non-cooperative localization networks can be treated as a special case of cooperative ones with $\mathbf{C}_{ij} = \mathbf{0}$ in (6).

SPEB characterizes the fundamental limit of localization accuracy, and provides valuable performance benchmarks and insights to the system design. Furthermore, SPEB is a tight bound (achievable) in high SNR regimes. So we choose SPEB as the performance metric for location-aware networks in our work.

## III. Optimal JPBA in Synchronous Networks

In this section, we start with the optimal JPBA problem in synchronous cooperative localization networks, where all agents and anchors work with perfectly synchronized clocks.

### A. Range Information Intensity

Based on the definition of SPEB, RII plays an important role in localization accuracy problems. In synchronous networks, range information between node $k$ and $j$ can be obtained by OWR

$$\hat{d}_{kj} = c\,\Delta t \tag{10}$$

where $c$ is the speed of light in free space, and $\Delta t$ is the TOA measurement results.

*Proposition 1:* The RII in synchronous networks using OWR can be represented as

$$\lambda_{kj} = \xi_{kj} \frac{P_k \beta_k^2}{d_{kj}^{\varrho}} \tag{11}$$

where $\xi_{kj}$ is called *ranging channel gain* (RCG) between node $k$ and $j$, $\varrho$ indicates the pathloss coefficient, and $P_k$ and $\beta_k$ are

normalized power and effective bandwidth allocated to node $k$ during measurements.

*Proof:* See the Appendix.

*Remark 1:* We consider the modulated communications systems in this paper, where the carrier phase information is not exploited for TOA estimation [30]. In such a case, the effective bandwidth is equivalent (or proportional) to the real signal bandwidth if the baseband signal waveform is suitably chosen (e.g., sinc-shaped pulses). Nevertheless, when fully coherent reception is applied, the contribution of carrier information is another major factor to be considered for TOA estimation [31].

According to Proposition 1, global SPEB in (7) can be represented as the function of normalized power and bandwidth allocation, which are the main resources to be optimized.

### B. Single Time Slot JPBA Formulation

We first consider only one time slot available for localization in the network, which implies that all measurements have to be performed simultaneously. Global SPEB is considered as the objective function to be minimized. Normalized power and bandwidth allocation solutions among all nodes to be optimized can be represented as $(N_\mathrm{a} + N_\mathrm{b}) \times 1$ vectors,

$$\mathbf{P} = [P_1, P_2, \ldots, P_{N_\mathrm{a}+N_\mathrm{b}}]^\mathrm{T}, \quad \boldsymbol{\beta} = [\beta_1, \beta_2, \ldots, \beta_{N_\mathrm{a}+N_\mathrm{b}}]^\mathrm{T}. \quad (12)$$

The problem can be formulated as

$$\mathscr{P}_\mathrm{S}^1: \ \min. \ \sum_{k\in\mathcal{N}_\mathrm{a}} \mathcal{P}\big(\mathbf{p}_k; \{P_i, \beta_i\}\big) \quad (13)$$

$$\text{s.t.} \quad 0 \le P_i \le P_0 \ \text{ and } \ 0 \le \beta_i \le B_0 \quad (14)$$

$$\sum_{i\in\mathcal{N}_\mathrm{a}\cup\mathcal{N}_\mathrm{b}} P_i \le P_\mathrm{total} \quad (15)$$

$$\sum_{i\in\mathcal{N}_\mathrm{a}\cup\mathcal{N}_\mathrm{b}} \beta_i \le B_\mathrm{total}. \quad (16)$$

Constraint (14) shows that each node has an upper limit on transmission bandwidth $B_0$ and peak power constraint $P_0$ due to the hardware design. Constraint (15) gives the upper bound of total power ($P_\mathrm{total}$). This constraint is derived from the interference point of view, which reflects the amount of overall interference transmitted. Constraint (16) is added to avoid frequency overlaps among different nodes. All nodes are assumed to work on the same carrier frequency, which implies $B_\mathrm{total} = B_0$ in this formulation.

Note that, SPEB is essentially determined by many network parameters which are unknown, such as the positions of agents and channel properties. In this paper, we assume all related parameters are known beforehand. So $\mathscr{P}_\mathrm{S}^1$ and problems formulated later are called "optimal" JPBA problems, by which the performance benchmarks can be obtained. However, in realistic location aware networks, we need to obtain these parameters first. For example, the channel parameters can be obtained by various types of maximum-likelihood estimators [32] or sparse estimation algorithms [33]. Due to the uncertainties of these network parameters, the "robust" JPBA frameworks (based on the "optimal" ones) are thus required to handle this issue in the future. Some related solutions can be found in [31] and [34].

### C. Multiple Time Slots JPBA Formulation

The single time slot framework can be easily extended to the multiple time slots scenario, which is a *static* network scheduling optimization problem. If there are $N_\mathrm{t}$ time slots available, the resource allocation solutions will extend to $(N_\mathrm{a} + N_\mathrm{b}) \times N_\mathrm{t}$ matrices instead of vectors in (12). The set of time slots is represented by $\mathcal{N}_\mathrm{t} = \{1, 2, \ldots, N_\mathrm{t}\}$. Power and bandwidth of node $i$ at time slot $t$ are denoted by $P_{i,t}$ and $\beta_{i,t}$, respectively. Compared to the single slot scenario, the peak and total power constraints are similar, and are rewritten as

$$0 \le P_{i,t} \le P_0 \quad (17)$$

$$\sum_{t=1}^{N_\mathrm{t}} \sum_{i=1}^{N_\mathrm{a}+N_\mathrm{b}} P_{i,t} \le P_\mathrm{total}. \quad (18)$$

Bandwidth allocation is different the single-slot scenario. An extra constraint on total bandwidth available is required, which is $B_\mathrm{total} = N_\mathrm{t} B_0$. In each time slot, the related bandwidth constraints are the same as problem $\mathscr{P}_\mathrm{S}^1$. Bandwidth constraints are summarized as follows

$$0 \le \beta_{i,t} \le B_0 \quad \forall i, t \quad (19)$$

$$\sum_{i=1}^{N_\mathrm{a}+N_\mathrm{b}} \beta_{i,t} \le N_\mathrm{t} B_0 \quad \forall t \quad (20)$$

$$\sum_{t=1}^{N_\mathrm{t}} \sum_{i=1}^{N_\mathrm{a}+N_\mathrm{b}} \beta_{i,t} \le N_\mathrm{t} B_0. \quad (21)$$

Therefore, the problem formulation for multiple time slots is

$$\mathscr{P}_\mathrm{S}^2: \ \min. \ \sum_{k\in\mathcal{N}_\mathrm{a}} \mathcal{P}(\mathbf{p}_k; \{P_{i,t}, \beta_{i,t}\})$$
$$\text{s.t.} \quad (17) - (21).$$

### D. Different JPBA Schemes

To simplify the notation, $P_\mathrm{anchor}$, $B_\mathrm{anchor}$, $P_\mathrm{agent}$ and $B_\mathrm{agent}$ are henceforth used to represent the sum of power and bandwidth resources for anchors and agents, respectively

$$\sum_{t=1}^{N_\mathrm{t}} \sum_{k=1}^{N_\mathrm{a}} P_{k,t} = P_\mathrm{agent}, \sum_{t=1}^{N_\mathrm{t}} \sum_{k=1}^{N_\mathrm{a}} \beta_{k,t} = B_\mathrm{agent}$$
$$\sum_{t=1}^{N_\mathrm{t}} \sum_{j=1}^{N_\mathrm{b}} P_{j,t} = P_\mathrm{anchor}, \sum_{t=1}^{N_\mathrm{t}} \sum_{j=1}^{N_\mathrm{b}} \beta_{j,t} = B_\mathrm{anchor}.$$

The single slot scenario is treated as a special case with $N_\mathrm{t} = 1$. Constraints in $\mathscr{P}_\mathrm{S}^1$ and $\mathscr{P}_\mathrm{S}^2$ can be rewritten as

$$P_\mathrm{anchor} + P_\mathrm{agent} \le P_\mathrm{total} \quad (22)$$

$$B_\mathrm{anchor} + B_\mathrm{agent} \le B_\mathrm{total} \quad (23)$$

$$0 \le P_{k,t} \le P_0, \ 0 \le \beta_{k,t} \le B_0 \quad (24)$$

which is named as a fully flexible (FF) allocation scheme in this paper.

Based on the constraints in the FF scheme, four more allocation schemes may be attained by introducing extra constraints.

- Power flexible scheme (PF). In PF, besides the global constraints (22) - (24), a constraint on the bandwidth allocation on $B_{\text{anchor}}$ and $B_{\text{agent}}$ is given, i.e.,
$$B_{\text{anchor}} = B_{\text{agent}} = \frac{1}{2}B_{\text{total}}. \tag{25}$$
- Bandwidth flexible scheme (BF). Similar to PF, an extra constraint on power allocation is added.
$$P_{\text{anchor}} = P_{\text{agent}} = \frac{1}{2}P_{\text{total}}. \tag{26}$$
- Equally allocation scheme (EA). Both constraints on power and bandwidth (25) - (26) are added.
- Purely uniform allocation scheme (PUA). Each node is allocated the same amount of resources, i.e.,
$$P_i = \frac{1}{N_{\text{a}}+N_{\text{b}}}P_{\text{total}} \quad \text{and} \quad \beta_i = \frac{1}{N_{\text{a}}+N_{\text{b}}}B_{\text{total}}.$$

These schemes give different constraints on the resource allocation for further evaluation. A special case of PF is to set $B_{\text{total}} = 2B_0$. Then measurements by anchors and agents are carried out in two individual time slots, respectively. In EA, it means that the agents' cooperation is regarded to be as important as anchors. Since anchors usually provide higher localization accuracy due to their known positions, the scheme is less efficient. However, the extra constraints make the optimization problem much simpler to solve, as the anchor optimization and agent optimization can be performed separately. PUA is not an optimized resource allocation scheme, and is only used for performance comparison here.

## IV. Optimal JPBA in Asynchronous Networks

The perfect synchronization assumption is often not fulfilled in wireless networks. We thus also consider an asynchronous scenario, where the problem formulation is different. Round trip measurements (RTM) are applied for range estimation where a minimum of two time slots is required.[2] Correspondingly, the network scheduling strategy is firstly described, based on which the resource allocation problems can be formulated.

In the first time slot, measurements are initiated by agents in a broadcast way. After that, in order to fulfill the RTM, anchors and selected *cooperative* agents are allowed to reply in the second time slot (small time stamps are attached for different processing time $\Delta t$ for each agent). Due to the practical half-duplex transceivers, agents are permitted to simultaneously transmit and receive signals only on different frequency bands. Therefore, range information not only between the agent and anchors, but also among different agents can be achieved.

[2]Timing accuracy required for ranging is extremely high (on the order of nanoseconds). However, time slots division (on the millisecond order) can be easily achieved by existing synchronization methods in communications networks. However, they are still treated as asynchronous networks for ranging and localization.

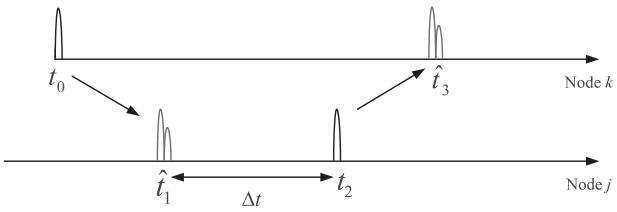


Fig. 3. Range estimation by the round trip measurement of impulse radio signals.

### A. Asynchronous RII

As shown in Fig. 3, in asynchronous networks, range information between node $k$ and $j$ can be obtained by round trip measurements,

$$\hat{d} = \frac{c}{2}[(\hat{t}_3 - t_0) - (t_2 - \hat{t}_1)] \tag{27}$$

where $\hat{t}_3$ and $\hat{t}_1$ are TOA estimation results by node $k$ and $j$. Therefore, the error variance of $\hat{d}$ can be obtained by

$$\sigma_{\text{d}}^2 = \frac{c^2}{4}(\sigma_3^2 + \sigma_1^2) = \frac{1}{4}(\frac{1}{\lambda_{jk}} + \frac{1}{\lambda_{kj}}) \tag{28}$$

where $\lambda_{kj}$ is RII by OWR from node $k$ to node $j$ defined in (11).

Since the measurement on link $k$ to $j$ is symmetric, we have $\xi_{kj} = \xi_{jk}$ and $d_{kj} = d_{jk}$. Asynchronous RII ($\tilde{\lambda}_{kj}$) of RTM in (28) can thus be rewritten as

$$\tilde{\lambda}_{kj} = \frac{1}{\sigma_{\text{d}}^2} = \xi_{kj}\frac{4P_{k,1}\beta_{k,1}^2 P_{j,2}\beta_{j,2}^2}{d_{kj}^{\varrho}(P_{k,1}\beta_{k,1}^2 + P_{j,2}\beta_{j,2}^2)}. \tag{29}$$

### B. Optimal JPBA Formulation in Different Schemes

If there are only the minimally required two time slots available , i.e., $\mathcal{N}_{\text{t}} = \{1, 2\}$, all nodes are generally allowed to transmit signals in both time slots. Similar to the synchronous scenario, the individual and interference constraints still hold in this section, i.e.,

- Individual constraints. Each node has an upper limit on transmission bandwidth $B_0$ and peak power $P_0$.
$$\beta_{i,t} \le B_0 \quad \text{and} \quad P_{i,t} \le P_0, \quad i \in \mathcal{N}_{\text{a}} \cup \mathcal{N}_{\text{b}} \quad t \in \mathcal{N}_{\text{t}}. \tag{30}$$
- Interference constraints. In each time slot, in order to avoid interferences to the receivers, transmission bands from all nodes are not allowed overlap.
$$\sum_{j=1}^{N_{\text{b}}}\beta_{j,1} + \sum_{k=1}^{N_{\text{a}}}\beta_{k,1} \le B_0 \tag{31}$$
$$\sum_{j=1}^{N_{\text{b}}}\beta_{j,2} + \sum_{k=1}^{N_{\text{a}}}\beta_{k,2} \le B_0. \tag{32}$$
- Global power constraints. Two different schemes are considered here. For non-power flexible (NPF) scheme, agents and anchors have their own total power constraints ($P_{\text{agent}}$ and $P_{\text{anchor}}$) respectively. On the other hand, there

is only one total power constraint ($P_{\text{total}}$) in the power flexible (PF) scheme. Therefore, in NPF, the total power constraints should be

$$\sum_{t=1}^{2}\sum_{k=1}^{N_{\text{a}}} P_{k,t} \le P_{\text{agent}} \tag{33}$$

$$\sum_{t=1}^{2}\sum_{j=1}^{N_{\text{b}}} P_{j,t} \le P_{\text{anchor}}. \tag{34}$$

In the PF scheme, the global power constraints should be

$$\sum_{t=1}^{2}\sum_{k=1}^{N_{\text{a}}} P_{k,t} + \sum_{t=1}^{2}\sum_{j=1}^{N_{\text{b}}} P_{j,t} \le P_{\text{total}}. \tag{35}$$

Based on the presented scheduling strategy, the asynchronous optimal JPBA problem modeling can thus be simplified, i.e., agents are allowed to transmit in both time slots, while anchors are only active in the second time slot, i.e.,

$$P_{j,1} = \beta_{j,1} = 0, \quad j \in \mathcal{N}_{\text{b}}. \tag{36}$$

A special case of the non-cooperative localization is realized by setting following constraints

$$P_{j,1} = \beta_{j,1} = 0, \quad j \in \mathcal{N}_{\text{b}} \tag{37}$$

$$P_{k,2} = \beta_{k,2} = 0, \quad k \in \mathcal{N}_{\text{a}}. \tag{38}$$

Global SPEB is still applied as the objective function. The cooperative JPBA problem in PF schemes is formulated as

$$\mathscr{P}_{\text{A}}^{1}: \ \min. \quad \sum_{k\in\mathcal{N}_{\text{a}}} \mathcal{P}(\mathbf{p}_k, \{P_{i,t}, \beta_{i,t}\})$$
$$\text{s.t.} \quad (30)-(32),\ (35),\ (36).$$

The NPF problem $\mathscr{P}_{\text{A}}^{2}$ can be obtained by replacing (35) with (33) and (34) in $\mathscr{P}_{\text{A}}^{1}$. Similarly, the counterparts in the non-cooperative scenario can be further obtained by replacing constraint (36) with (37) and (38) in $\mathscr{P}_{A}^{1}$ and $\mathscr{P}_{\text{A}}^{2}$.

Unfortunately, the JPBA problem with multiple time slots ($N_{\text{t}} > 2$) in asynchronous localization networks is complicated, and essentially NP-hard. Unlike the synchronous scenario, there does not exist a general optimal scheduling strategy. Some preliminary works can be found in [35] and [36]. This problem will be addressed in our future work.

## V. Optimization Algorithms

### A. A Trust Region Framework for Nonconvex Approximation

Although the constraints in all problems above are affine, JPBA optimizations in synchronous and asynchronous networks ($\mathscr{P}_{\text{S}}$ and $\mathscr{P}_{\text{A}}$) are both nonconvex due to the objective functions. We have to depend on techniques designed for nonconvex optimization which do not lead to the global optimal solution in most cases [37]. A reliable and robust framework for nonconvex approximation is called *Trust Region*, by which the original problem is approximated and solved with a sequence of convex problems. The trust region algorithms can even be applied to ill-conditioned problems, and proved to have very strong convergence properties [38]–[40].

The key idea of the trust region framework is that, the approximate model is only "trusted" in a region near the current iterate. For example, at the $m^{\text{th}}$ iteration, the nonconvex function $f(\boldsymbol{\theta})$ is approximated as

$$f(\boldsymbol{\theta}^{(m)}) = \tilde{f}(\boldsymbol{\theta}^{(m)})$$
$$||\boldsymbol{\theta}^{(m)} - \boldsymbol{\theta}^{(m-1)}||_2 \le R^{(m)} \tag{39}$$

where $\tilde{f}(\boldsymbol{\theta})$ is the convex approximation, and $\boldsymbol{\theta}^{(m-1)}$ is the solution obtained in the $m-1^{\text{th}}$ iteration, which is applied as the starting point in the next iteration. Parameter $R^{(m)}$ is the trust region radius at current iteration, which is usually determined by the $\ell$-2 norm.

In trust region algorithms, one important issue is to decide the trust region trial step and whether a trial step should be accepted. The predicted reduction $P_{\text{red}}^{(m)}$ and actual reduction $A_{\text{red}}^{(m)}$ at $m^{\text{th}}$ iteration are defined respectively

$$P_{\text{red}}^{(m)} = |\tilde{f}(\boldsymbol{\theta}^{(m)}) - \tilde{f}(\boldsymbol{\theta}^{(m-1)})|$$
$$A_{\text{red}}^{(m)} = |f(\boldsymbol{\theta}^{(m)}) - f(\boldsymbol{\theta}^{(m-1)})|.$$

The ratio between $P_{\text{red}}^{(m)}$ and $A_{\text{red}}^{(m)}$ is defined as

$$\mu^{(m)} = \frac{P_{\text{red}}^{(m)}}{A_{\text{red}}^{(m)}}. \tag{40}$$

By comparing to a preset threshold, $\mu^{(m)}$ is applied to decide whether the trial step is acceptable and to adjust the new trust region radius. Generally speaking, if $\mu^{(m)}$ indicates that the approximate model fits the original problem well, the trust region can be enlarged. Otherwise, the trust region should be reduced. More details about the trust region frameworks can be found in [38], [40], and references therein.

### B. Taylor Linearization Method

In this section, a Taylor linearization (TL) approximation method based on the trust region framework is presented to solve the asynchronous JPBA problems.[3] Synchronous problems ($\mathscr{P}_{\text{S}}^{1}$ and $\mathscr{P}_{\text{S}}^{2}$) can be treated as special cases and solved accordingly.

In $\mathscr{P}_{\text{A}}^{1}$ and $\mathscr{P}_{\text{A}}^{2}$, only the objective functions are nonconvex due to the asynchronous RII ($\tilde{\lambda}_{kj}$) in (29). According to the trust region framework, we perform Taylor linearization on $\tilde{\lambda}_{kj}$ around a certain expansion point, and then. $\tilde{\lambda}_{kj}$ can be rewritten as (41), shown at the bottom of this page, combined with two trust region constraints

$$||\mathbf{P} - \mathbf{P}^{(m-1)}|| = ||\Delta\mathbf{P}|| \le R_{\mathbf{P}}^{(m)} \tag{42}$$

$$||\boldsymbol{\beta} - \boldsymbol{\beta}^{(m-1)}|| = ||\Delta\boldsymbol{\beta}|| \le R_{\boldsymbol{\beta}}^{(m)}. \tag{43}$$

[3]Here we take the PF scheme for example, while NPF can be treated as a special case of PF.

$$\tilde{\lambda}_{kj}(\mathbf{P}, \boldsymbol{\beta}) \approx \tilde{\lambda}_{kj}^{\text{TL}}(\mathbf{P}, \boldsymbol{\beta}) = \tilde{\lambda}_{kj}(\mathbf{P}^{(m-1)}, \boldsymbol{\beta}^{(m-1)}) + \nabla_{\mathbf{P}}\tilde{\lambda}_{kj}(\mathbf{P}^{(m-1)})\Delta\mathbf{P} + \nabla_{\boldsymbol{\beta}}\tilde{\lambda}_{kj}(\boldsymbol{\beta}^{(m-1)})\Delta\boldsymbol{\beta} \tag{41}$$

**Algorithm 1** A TL-Based Iterative Approximate Algorithm

1: Starting point selection. $\mathbf{P} = \mathbf{P}^{(0)}$, $\boldsymbol{\beta} = \boldsymbol{\beta}^{(0)}$, $m = 0$.
2: **while** convergence not satisfied
3: Solve the problem $\mathscr{P}_{\mathrm{A}}^{3}$. **Output**: $\Delta\mathbf{P}$ and $\Delta\boldsymbol{\beta}$.
4: Solution update: $\mathbf{P}^{(m+1)}$ and $\boldsymbol{\beta}^{(m+1)}$ according to $\mu^{(m)}$.
**if** $\mu^{(m)} < \mu_1$
$\mathbf{P}^{(m+1)} = \mathbf{P}^{(m)}$, $\boldsymbol{\beta}^{(m+1)} = \boldsymbol{\beta}^{(m)}$
**else**
$\mathbf{P}^{(m+1)} = \mathbf{P}^{(m)} + \Delta\mathbf{P}$, $\boldsymbol{\beta}^{(m+1)} = \boldsymbol{\beta}^{(m)} + \Delta\boldsymbol{\beta}$
**end**
5: Trust region radius update.
**if** $\mu^{(m)} < \mu_1$
$R_{\mathbf{P}}^{(m+1)} = c_1||\Delta\mathbf{P}||$, $R_{\boldsymbol{\beta}}^{(m+1)} = c_1||\Delta\boldsymbol{\beta}||$
**else if** $\mu^{(m)} > \mu_2$
$R_{\mathbf{P}}^{(m+1)} = \min\{c_2 R_P^{(m)}, R_P^{\star}\}$,
$R_{\boldsymbol{\beta}}^{(m+1)} = \min\{c_2 R_{\beta}^{(m)}, R_{\beta}^{\star}\}$
**else**
$R_{\mathbf{P}}^{(m+1)} = ||\Delta\mathbf{P}||$, $R_{\boldsymbol{\beta}}^{(m+1)} = ||\Delta\boldsymbol{\beta}||$
**end**
6: Convergence checking. $m = m + 1$.
7: **end**
8: **Output**: Optimal $\mathbf{P}$ and $\boldsymbol{\beta}$, Minimized SPEB.

By inserting $\tilde{\lambda}_{kj}^{\mathrm{TL}}$ into (8) and (9), an approximate SPEB ($\mathcal{P}^{\mathrm{TL}}(\mathbf{p}_k, \{\Delta\mathbf{P}, \Delta\boldsymbol{\beta}\})$) under Taylor linearization is attained.

Regarding the PF-JPBA problem $\mathscr{P}_{\mathrm{A}}^{1}$, an alternative form by Taylor linearization is

$$\mathscr{P}_{\mathrm{A}}^{3}: \ \min. \quad \sum_{k\in\mathcal{N}_{\mathrm{a}}} \mathcal{P}^{\mathrm{TL}}(\mathbf{p}_k, \{\Delta\mathbf{P}, \Delta\boldsymbol{\beta}\})$$
$$\text{s.t.} \quad (30)-(32),\ (35)-(36),\ (42)-(43).$$

*Proposition 2:* Problem $\mathscr{P}_{\mathrm{A}}^{3}$ is convex in $\Delta\mathbf{P}$ and $\Delta\boldsymbol{\beta}$.

*Proof*: The constraints in $\mathscr{P}_{\mathrm{A}}^{3}$ are affine, only the convexity of objective function is required here. Based on the rules of convex analysis, the convexity is closed under composition with an affine mapping [37]. Since the function $\mathrm{tr}\{\mathbf{X}^{-1}\}$ is convex when $\mathbf{X} \succ 0$, and RII ($\tilde{\lambda}_{kj}^{\mathrm{TL}}(\mathbf{P}, \boldsymbol{\beta}\})$) is joint affine in $\Delta\mathbf{P}$ and $\Delta\boldsymbol{\beta}$ after Taylor linearization, problem $\mathscr{P}_{\mathrm{A}}^{3}$ thus is proved convex.

According to the trust region framework, the trust radius and solutions are updated in an adaptive way based on the predictive quality ($\mu^{(m)}$) after $m^{\mathrm{th}}$ iteration.

- If the approximate model ($\mathcal{P}^{\mathrm{TL}}$) predicts the actual improvement well, or if there is even more improvement, we increase the radius $R^{(m)}$ and allow a longer step at the next iteration.
- If the model does a bad job in predicting, we decrease the size of the trust region in the next iteration, and recalculate $\Delta\theta$. Repeat this iteration step with the updated smaller trust region.
- Finally, if the model does an acceptable job of predicting the improvement in $\mathcal{P}$, we keep the size of the trust region.

An iterative approximation algorithm based on Taylor linearization is given in Algorithm 1. Since the JPBA problems are essentially nonconvex, only local convergence can be guaranteed. Therefore, we can run the approximation algorithm from multiple initial points and take the best result as the final solution [41]. At step 1 of Algorithm 1, two different starting points are thus considered in Algorithm 1.

1) Starting point 1 provides uniform allocation to the anchor nodes, while not providing any power to the agent nodes.
2) Starting point 2 provides an equal amount of resources to all anchor and agent nodes.

We choose positive constants $\mu_1 < \mu_2 < 1$ and $c_1 < 1$, $c_2 > 1$. Usually $\mu_1$ is small positive to keep any computed "good" points. Typically values for $\mu_1$ and $\mu_2$ are $\mu_1 = 0.10$ and $\mu_2 = 0.75$ [39]. $R_{\mathbf{P}}^{\star}$ and $R_{\boldsymbol{\beta}}^{\star}$ are the preset trust radius upper bounds of power and bandwidth, respectively.

In step 6, if the relative difference between SPEB achieved in the previous and current steps is small enough (compared to a preset threshold $\epsilon$), the iteration ends.

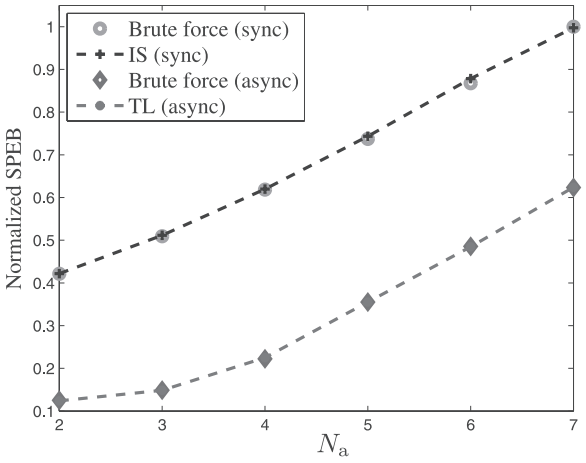


Fig. 4. Results comparison to the brute force search.

### C. Accuracy Evaluations of TL

Since the optimal JPBA problems are essentially nonconvex, the accuracy of the approximate algorithm is evaluated by comparisons to a (time consuming) brute force search. We first perform uniform JPBA among anchors. Optimal JPBA among agents are then achieved by TL and brute force respectively. Note that the solution might be inferior to the solution of the FF scheme; we present this example here purely to evaluate the accuracy of our solution methods.

Note that the global optimum *cannot be guaranteed by TL*. But it can be seen from Fig. 4 that, the accuracy achieved by TL is close to the brute force method. On the other hand, TL is much more computationally efficient, which makes it an appropriate option to optimal JPBA problems in both synchronous and asynchronous localization networks.

## VI. Numerical Results

### A. Network Settings

In this section, we present numerical examples for the localization performance based on the proposed JPBA schemes. A typical ranging scenario using impulse radio UWB signals (CM1 in IEEE 802.15.4a channel model [42]) is considered to

TABLE I
TYPICAL PARAMETERS IN UWB RANGING

| $W$ | $\nu$ | $\bar{\gamma}_{\mathrm{DP}}$ | $\bar{\chi}_{k_{ij}}$ | Power spectral density | $N_0$ |
|---|---|---|---|---|---|
| 500 (MHz) | 0.1 (m) | 0.2 | 0.32 | -41.3 (dBm/MHz) | -174 (dBm/Hz) |

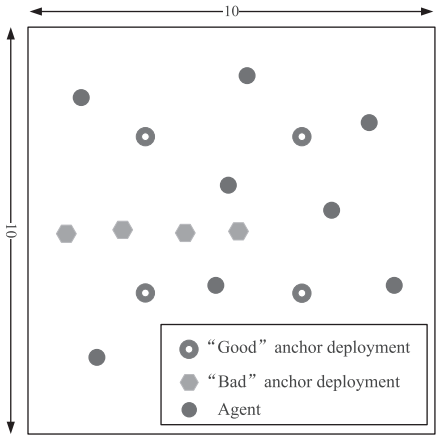


Fig. 5. The location-aware network consisting four anchors and multiple agents, where anchors are deployed in two different ways.

make the results more intuitive. A 2ns duration Gaussian pulse occupying 3.1-3.6GHz spectrum is used as the transmit waveform. The amplitude fading $\varphi_k$ is normalized here. An average RCG between two nodes can be obtained based on the practical parameters in Table I as $\bar{\xi} \approx 152.3$dB by (11). After that, global power ($P_{\mathrm{total}}$) and bandwidth ($B_{\mathrm{total}}$) constraints are normalized. Peak power and bandwidth constraints on each node are $P_0 = 0.4$, $B_0 = 1$ respectively. The path loss and shadowing are considered as the channel gains. Path loss coefficient is set as $\varrho = 2$. TL approach is applied to solve the JPBA problems, in which the two starting points described in Section V-B are investigated. The SPEB convergence rule is applied and the threshold for checking is $\epsilon = 10^{-3}$. The trust region upper bound is set as 0.5 for both $R^{\star}_{\mathbf{P}}$ and $R^{\star}_{\boldsymbol{\beta}}$. $\mu_1 = 0.10$ and $\mu_2 = 0.75$, $c_1 = 0.5$, $c_2 = 1.5$. In synchronous networks, both single and multiple time slots scenarios are considered, while only the two time slot scenario is evaluated in asynchronous networks, as discussed before.

A dense network example is shown in Fig. 5. There are $N_{\mathrm{b}} = 4$ prelocated anchors and $N_{\mathrm{a}}$ agents distributed in a square region, i.e., $U([0, 10] \times [0, 10])$. Adding agents increases the node density. It is widely recognized (see, e.g., [30]) that a good anchor deployment (AP) is on the vertices of a convex hull of the agent positions, to minimize errors. However, note that practical constraints may prevent such a placement. Thus, investigating the effect of AP on global accuracy and agents cooperation is important. For this purpose, we henceforth investigate two different APs shown in Fig. 5, and simply called "good" and "bad" AP.

### B. Synchronous Networks

*1) Single Time Slot Scenario:* We first consider the synchronous scenario with "good" AP in Fig .5. All five cooperative JPBA schemes proposed in Section III-D are implemented and evaluated for their accuracy. It can be seen that

- Total errors of all schemes increase with the number of agents. The main reason for that is the constraints on total power and bandwidth. Similar results are drawn in the non-cooperative scenario with optimal power allocation schemes [22].
- As we predicted in Section III, PUA is the simplest but least efficient scheme, since there is no optimization among resources.
- Compared among the four schemes other than PUA, FF performs best while EA is the worst. This is intuitive, since under constraint for the total resources, more flexibility offers better performance. The power and bandwidth resources can be automatically concentrated in the most helpful nodes, especially when there are no external constraints on it.
- We furthermore observe that BF outperforms PF. The reason is that EFIMs are affected by the square of the bandwidth, $P_j \beta_j^2$, and so bandwidth plays a more important role for the overall accuracy. Another reason is that, there exists an additional peak power constraint ($P_0 < P_{\mathrm{total}}$), which makes the PF scheme actually not completely flexible for power allocation.

Note that the errors shown here, which are in the sub-millimeter range, might not be easy to achieve in practice (similar to [43]). They are predicated on the ideal assumption that full channel state information is obtained, perfect sampling and quantization processing is attained, etc. Evaluations with practical algorithms using measured channel impulse responses (e.g., [44]) show errors that can be orders of magnitude larger. Nevertheless, the optimization frameworks in this paper still hold. Meaningful performance benchmarks and optimal cooperation strategies are provided thereby.

The gain obtained from agents' cooperation is another important issue. In Fig. 6(a), it is obvious that cooperation among agents is able to improve the accuracy in all schemes, but by different amounts. Cooperation is of great help to the performance in PF, when $B_{\mathrm{anchor}}$ is tightly restricted. On the other hand, cooperation gain in FF is quite limited. It means that, when anchors are properly deployed, the performance of non-cooperative localization in FF is close to the optimal solutions, while there is much a larger space for improvement for PF.

In the second scenario, cooperative JPBA solutions with shadowing and bad AP are studied. We use here a simplified shadowing model such that the SNR will decrease by 10 dB in case of a blockage between transmitter and receiver; the probability for such a blockage is $P_{\mathrm{shadowing}} = 0.5$. Due to the space restrictions, only FF is considered here. As shown in Fig. 6(b), it is observed that, when anchors are poorly deployed, cooperation plays a much more important role than in "good" AP scenarios, which agrees well with intuition. It is also obvious that "bad" AP leads to much larger localization errors; yet cooperation among agents will be able to mitigate the error effectively. Similarly, shadowing is an important factor that affects the performance. When anchors are severely blocked, they provide degraded ranging information to the

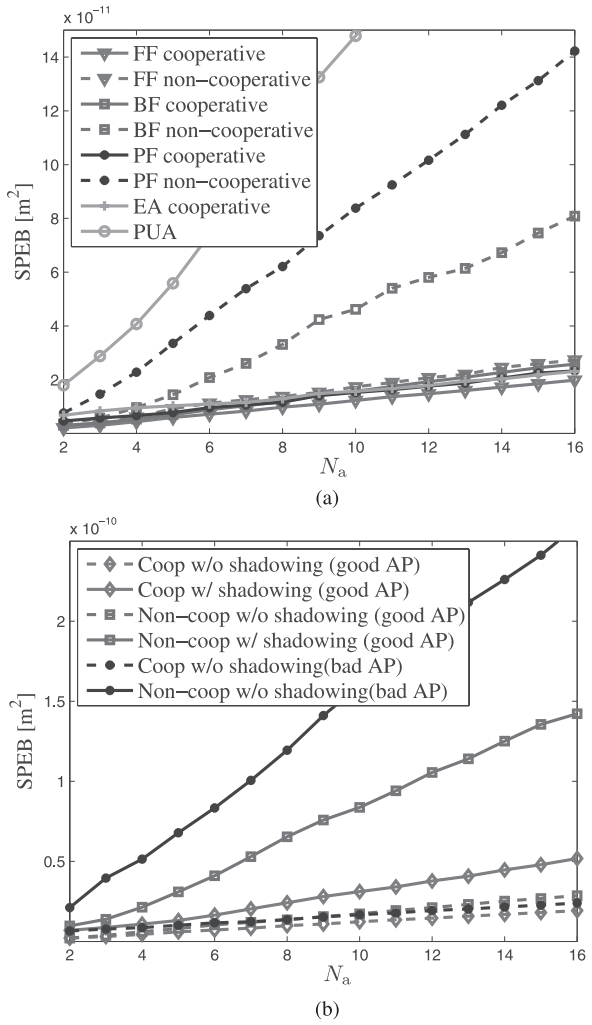


Fig. 6. SPEB results in single-time-slot synchronous networks. (a) Different schemes (in good AP) w/o shadowing. (b) Different channel conditions and APs.

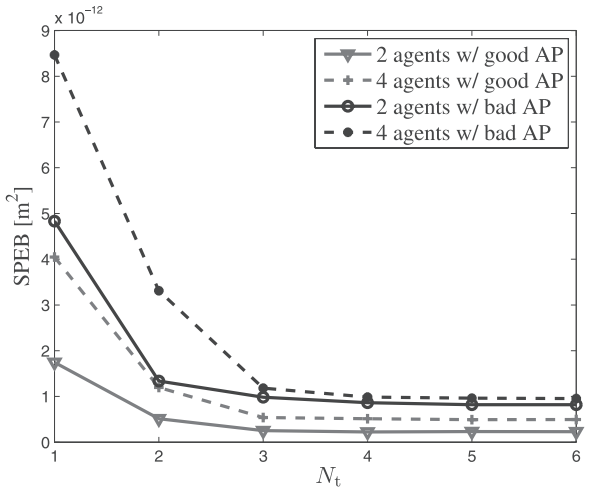


Fig. 7. SPEB results in multiple-time-slot synchronous networks.

agents and hence agent's cooperation plays a more important role in localization.

*2) Multiple Time Slots Scenario:* In this part, FF-JPBA with multiple time slots available are studied, where two and four agents are considered for localization performance evaluation. As shown in Fig. 7, accuracy becomes better with more time

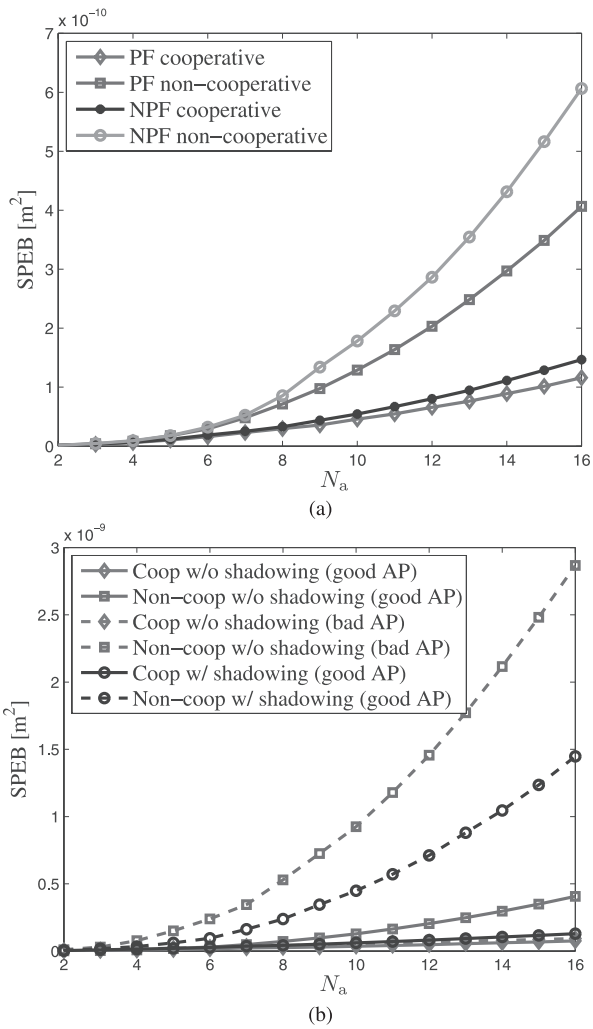


Fig. 8. SPEB results in asynchronous networks. (a) Different schemes (in good AP) w/o shadowing. (b) Different channel conditions and APs.

slots, which agrees with the previous analysis. However, when the number of time slots is more than 3, it shows that the accuracy remains at a certain level. The reason is that, although there are still lot of bandwidth resources available, power resources for measurements have been used up. It is equivalent to the pure power allocation strategy when $N_t$ is large enough for each node to perform individual measurements.

### *C. Asynchronous Networks*

In this section, the accuracy solutions in asynchronous networks with different schemes are studied. Both PF and NPF schemes are evaluated in Fig. 8(a). Shadowing effects and different APs are considered in Fig. 8(b). From the numerical results, it can be concluded that,

- Similar to the synchronous scenario, the total localization error increases with respect to the agent number.
- PF outperforms NPF in accuracy. Similar to the conclusions drawn in the synchronous scenario, more flexibility in resource allocation offers better performance.
- Channel and anchor deployment are still important factors on localization accuracy. When the anchor deployment or the channel condition is poor, cooperation among agents plays a much more important role than under ordinary conditions.

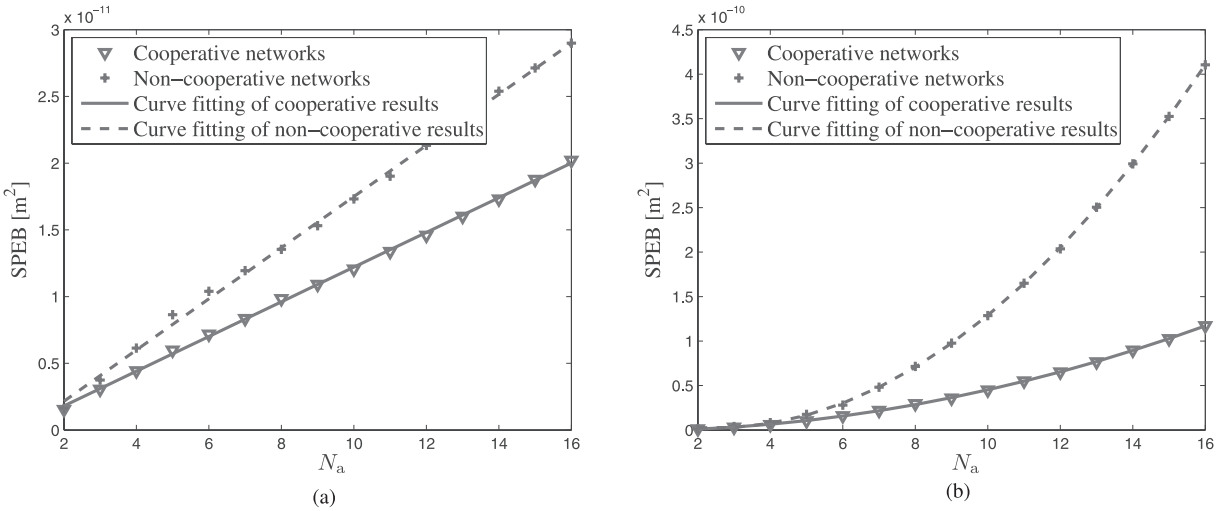


Fig. 9. Scaling analysis of synchronous and asynchronous networks. (a) Synchronous networks. (b) Asynchronous networks.

### *D. Discussions on Accuracy and Scaling Laws*

In this part, we first compare the accuracy between synchronous ($N_{\mathrm{t}} = 1$) and asynchronous ($N_{\mathrm{t}} = 2$) networks. It can be seen from Fig. 9, even though there are two time slots available in the asynchronous localization network (i.e. $B_{\mathrm{total}} = 2B_0$), accuracy performance in the synchronous scenario is much better.

Scaling laws for accuracy show the benefit of cooperation and synchronization in large networks. In Fig. 9, we perform least square (LS) curve fitting over the achieved results in both synchronous and asynchronous networks. It can be seen from Fig. 9(a), global SPEB scales proportional to the number of agents in synchronous networks ($\Theta(N_{\mathrm{a}})$), which implies the average SPEB in synchronous networks remains nearly constant when a new agent is added. The main reason is that, since we use a broadcast strategy, anchors play the main role in synchronous localization networks (which is also described in detail later in Section VI-E). New agents can generally localize themselves by the broadcasted signals from anchors without extra resources.

On the other hand, SPEB increases quadratically with respect to the number of agents, i.e., $\Theta(N_{\mathrm{a}}^2)$ in Fig. 9(b). It implies that the average SPEB scales as $\Theta(N_{\mathrm{a}})$ in asynchronous networks. According to the localization strategies in Section IV, all agents and anchors are required to transmit signals. Therefore, if new agents are added, the average resources allocated to each agent decreases proportionally, which leads to a SPEB increase along with the agent number.

Note that our analysis is based on a typical *dense* network. If the measurement is carried out in an *extended* network (network area increases proportional to the number of nodes), the scaling rules are quite different since the pathloss and therefore SNR changes.

### *E. Resource Allocation Solutions*

To analyze the resource allocation solutions, we first consider the optimal allocation ratio between anchors and agents. An auxiliary parameter is defined as

$$\zeta = \frac{P_{\mathrm{anchor}} B_{\mathrm{anchor}}^2}{P_{\mathrm{anchor}} B_{\mathrm{anchor}}^2 + P_{\mathrm{agent}} B_{\mathrm{agent}}^2} \tag{44}$$

which indicates the percentage of resources that are allocated to anchors.

Resource allocation solutions are different in synchronous and asynchronous networks due to the two ranging methods applied. As shown in Fig. 10, agents are kept quiet in synchronous non-cooperative measurements. All resources are used by the anchors, which leads to $\zeta = 1$. Fig. 10(a) shows different resource allocation solutions in synchronous networks. It suggests that when anchors are properly deployed and channel conditions are good, non-cooperative localization achieves close-to-optimum solutions. This conclusion also can be drawn from the FF solutions in Fig. 6(a) and Fig. 6(b). Therefore, most resources are recommended to be allocated to anchors. On the other hand, if anchors are poorly located and channel conditions are not so good, agents' cooperation will be increasingly important as the agents' number increases. Nevertheless, $\zeta$ is still suggested to be greater than 0.5. This agrees with the conclusions in [20] that anchors play the main role during localization in most cases. Another phenomenon is that, since there exists a peak power constraint $P_0 = 0.4$, $\zeta$ in PF is smaller than FF and BF.

In asynchronous networks, agents are required to perform transmission during each RTM, even if in a non-cooperative manner. Therefore, $\zeta$ will thus be much smaller than in the synchronous case. In Fig. 10(b), $\zeta \leq 0.5$ in most non-cooperative cases when $N_{\mathrm{a}} > 3$. A special case of asynchronous JPBA is non-cooperative NPF, where

$$P_{\mathrm{anchor}} = P_{\mathrm{agent}} = 0.5, \quad B_{\mathrm{anchor}} = B_{\mathrm{agent}} = 1$$

and the corresponding $\zeta$ is 0.5. When cooperation among agents is carried out, $\zeta$ is nearly 0.2 smaller than the corresponding non-cooperative $\zeta$. When the agent number is relative large, $\zeta$ is even smaller than 0.1. It implies that, in optimal cooperative asynchronous networks, most of the

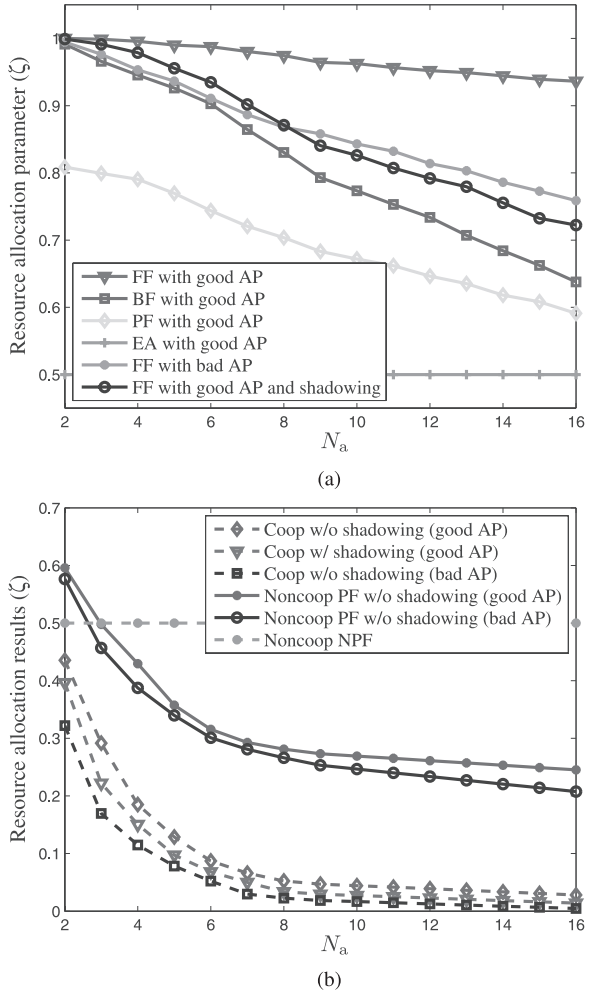


Fig. 10. Resource allocation solutions in different schemes. (a) Sync networks. (b) Async networks.

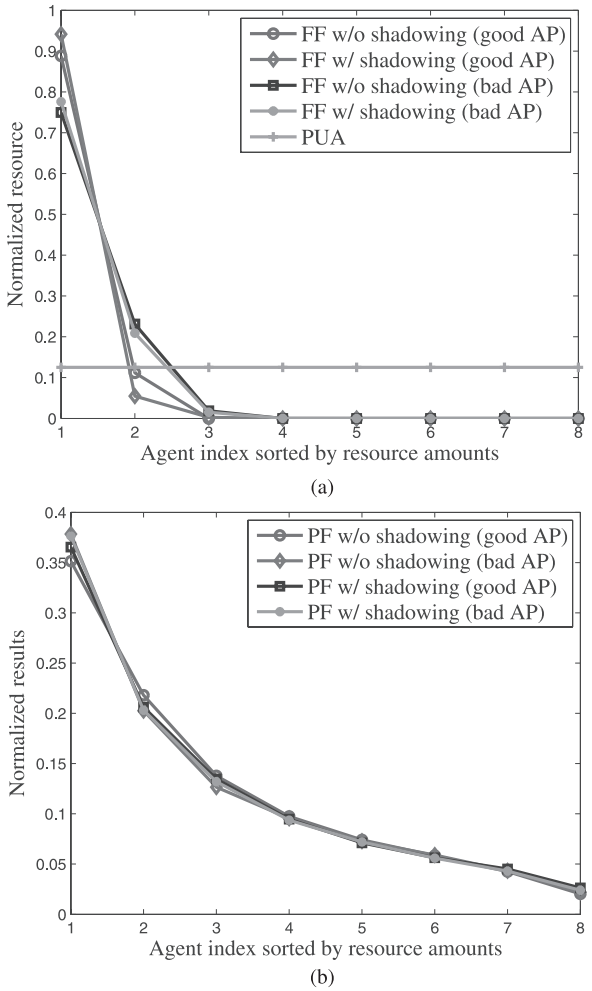


Fig. 11. Resource allocation solutions among cooperative agents. (a) Sync networks. (b) Async networks.

resources are allocated to the agents, which is different from the results drawn from the synchronous scenario.

Optimal resource distribution among agents is helpful to explain how the cooperation among agents works. Fig. 11 shows the resource allocation solutions among eight agents as an example. From Fig. 11(a), in contrast to PUA, all optimized JPBA schemes allocate the resources to the one or two most helpful agents, even in bad AP and shadowing conditions. In other words, the resource distribution among agents is extremely sparse, which is consistent with the power allocation solutions in [24].

However, the distribution of resources is different in the asynchronous networks. In Fig. 11(b), the resource allocation solutions are much more balanced than in Fig. 11(a). One main reason is that, agents must perform transmission during the RTM in both non-cooperative and cooperative localization. A uniform resource allocation strategy may be more suitable in asynchronous localization networks accordingly.

### *F. Moving-Agent Scenarios*

In this part, we consider another typical scenario in GPS-challenged environments. As shown in Fig. 12(a), five agents enter the square area from the left side as a group. Four anchors are prelocated at the vertices of the area. Both synchronous and asynchronous measurements are considered. Optimal JPBA is performed with the movement of the group. SPEB is obtained with respect to the position of the central agent. From the results in Fig. 12(b), some conclusions can be drawn.

- Localization accuracy with synchronization achieved is much better than that in the asynchronous network, which agrees with the results in Fig. 9. In the synchronous system, SPEB achieved by cooperative methods are only slightly better than the non-cooperative ones (e.g., results on $z = -1$ and $z = 11$, etc). But in asynchronous networks, cooperation among agents is able to promote the accuracy obviously in all investigated cases.
- Since the network topology is symmetric during the agents' movement, the solutions obtained are symmetric as well. When the agent group is far away from the anchor area, RII will be relatively small due to the pathloss, which leads to a large localization error.
- When the right two agents (1 and 2) approach the borderline (i.e., $z = -1$), anchor 1 and 2 are nearly on the same line with agents. This is problematic for localization due to the geometric deployment. Therefore, EFIM for localization is mainly provided by anchor 3 and 4, which are far away from the agent group. It leads to a SPEB

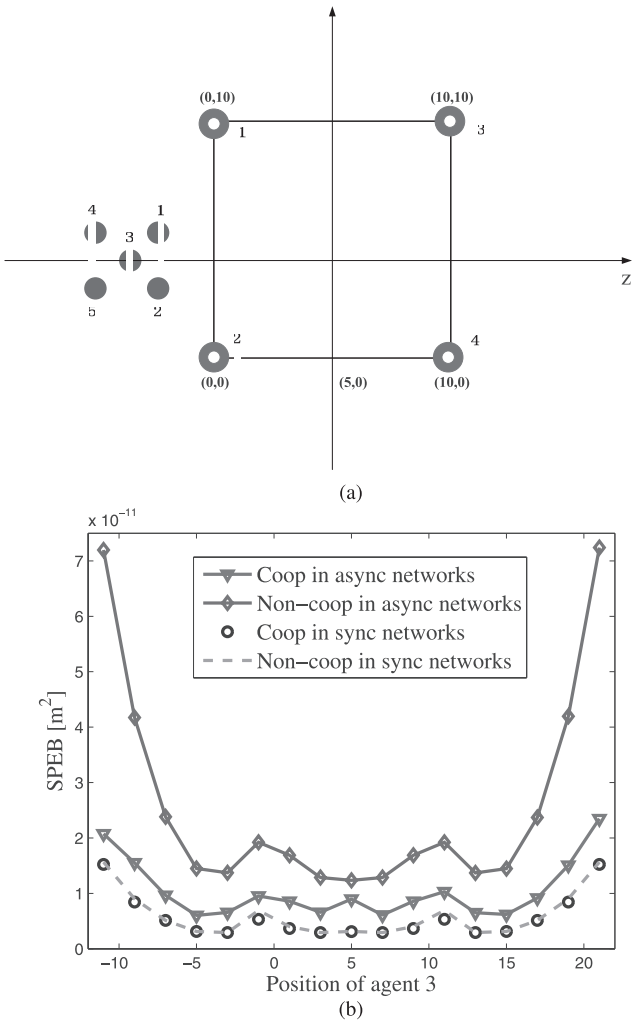


Fig. 12. Accuracy results in moving agents scenario. (a) Moving agents network. (b) Accuracy results with respect to the positions of agents.

peak at $z = -1$. The reason for another SPEB peak at $z = 11$ is similar.

## VII. Conclusion

In this paper, we formulated the optimization problems for resource allocation in cooperative localization systems, where both one-way and two-way ranging are considered. Since the optimization problems are nonconvex, we developed iterative linearization methods that provide efficient numerical solutions, and achieve near-optimal performances in the investigated case studies of simulations. From the simulation results, we can have the following important observations: (i) both bandwidth and power allocation among the nodes are important for good localization performance, where the former is more critical; (ii) cooperation among agents is especially important when anchor placement is bad, and/or severe shadowing occurs, (iii) the optimal resource allocation for one-way ranging is sparse, and (iv) for two-way ranging, the optimal resource allocation is more balanced. These algorithms developed in this paper and the insights obtained from the simulation results can facilitate the design and operation of efficient wireless localization networks.

## Appendix
## Proof of Proposition 1

In [29], the RII between node $k$ and $j$ is defined as

$$\lambda_{kj} = \frac{8\pi^2 \tilde{\beta}_k^2}{c^2}(1-\chi_{kj})\mathrm{SNR}_j^{(1)} \tag{45}$$

where $\chi_{kj} \in (0,1)$ is the path-overlap coefficient (POC) that characterizes the effect of multipath propagation for localization, $\tilde{\beta}_k$ is the real effective bandwidth of the transmitted waveform from node $k$, defined as

$$\tilde{\beta}_k = \Big(\frac{\int_{-\infty}^{\infty} f^2 |S_k(f)|^2 df}{\int_{-\infty}^{\infty} |S_k(f)|^2 df}\Big)^{1/2} \tag{46}$$

in which $S_k(f)$ is the spectrum of $s_k(t)$. In this paper, we assume that full channel parameters are known beforehand. So the amplitude fading $\varphi_k$ on $s_k(t)$ is known thereafter. Furthermore, $\mathrm{SNR}_j^{(l)}$ is the energy ratio between the $l^{\text{th}}$ multipath component and the noise at node $j$, i.e.,

$$\mathrm{SNR}_j^{(l)} \triangleq \frac{E_l}{N_0} = \frac{\tilde{P}_k |\alpha_j^{(l)}|^2 \int_0^{T_{\text{ob}}} |s_k(t)|^2 dt}{N_0} \tag{47}$$

where $\tilde{P}_k$ is the reference transmit power of node $k$ (measured at a reference distance, such as 1 meter away from the transmitter [45]). Since the energy of $s(t)$ is normalized, the energy of the transmitted waveform $s_k(t)$ can be represented as $\varphi_k^2$.

To simplify the notations, we define normalized power and effective bandwidth allocated to node $k$ as $P_k = \tilde{P}_k / P_{\text{peak}}$ and $\beta_k = \tilde{\beta}_k / W$, respectively. Here $P_{\text{peak}}$ and $W$ are peak values of power and effective bandwidth available on each node. We thus have the power of direct path (DP) component as

$$\tilde{P}_k |\alpha_j^{(1)}|^2 \varphi_k^2 = \gamma_{\text{DP}} \varphi_k^2 P_{\text{peak}} P_k$$

where $\gamma_{\text{DP}}$ is the ratio of DP power among all multipath components. RII $\lambda_{kj}$ can be rewritten as

$$\begin{aligned}\lambda_{kj} &= \frac{8\pi^2 W^2 (1-\chi_{kj}) \gamma_{\text{DP}} \varphi_k^2 P_{\text{peak}}}{c^2 N_0} \Big(\frac{\nu}{4\pi d_{\text{ref}}}\Big)^2 \Big(\frac{d_{\text{ref}}}{d_{kj}}\Big)^{\varrho} P_k \beta_k^2 \\ &= \xi_{kj} \frac{P_k \beta_k^2}{d_{kj}^{\varrho}}\end{aligned} \tag{48}$$

where $\nu$ is the wave length of the transmitted signals. The proof is thus complete.

## References

[1] M. Z. Win *et al.*, "Network localization and navigation via cooperation," *IEEE Commun. Mag.*, vol. 49, no. 5, pp. 56–62, May 2011.

[2] A. H. Sayed, A. Tarighat, and N. Khajehnouri, "Network-based wireless location: Challenges faced in developing techniques for accurate wireless location information," *IEEE Signal Process. Mag.*, vol. 22, no. 4, pp. 24–40, Jul. 2005.

[3] K. Pahlavan, X. Li, and J.-P. Mäkelä, "Indoor geolocation science and technology," *IEEE Commun. Mag.*, vol. 40, no. 2, pp. 112–118, Feb. 2002.

[4] S. Gezici *et al.*, "Localization via ultra-wideband radios: A look at positioning aspects for future sensor networks," *IEEE Signal Process. Mag.*, vol. 22, no. 4, pp. 70–84, Jul. 2005.

[5] D. Jourdan, D. Dardari, and M. Win, "Position error bound for UWB localization in dense cluttered environments," *IEEE Trans. Aerosp. Electron. Syst.*, vol. 44, no. 2, pp. 613–628, Apr. 2008.

[6] R. Niu and P. K. Varshney, "Target location estimation in sensor networks with quantized data," *IEEE Trans. Signal Process.*, vol. 54, no. 12, pp. 4519–4528, Dec. 2006.

[7] Y. Shen, S. Mazuelas, and M. Z. Win, "Network navigation: Theory and interpretation," *IEEE J. Sel. Areas Commun.*, vol. 30, no. 9, pp. 1823–1834, Oct. 2012.

[8] N. Patwari, J. N. Ash, S. Kyperountas, A. O. Hero, R. L. Moses, and N. S. Correal, "Locating the nodes: Cooperative localization in wireless sensor networks," *IEEE Signal Process. Mag.*, vol. 22, no. 4, pp. 54–69, Jul. 2005.

[9] H. Wymeersch, S. Maranò, W. M. Gifford, and M. Z. Win, "A machine learning approach to ranging error mitigation for UWB localization," *IEEE Trans. Commun.*, vol. 60, no. 6, pp. 1719–1728, Jun. 2012.

[10] S. Gezici and H. V. Poor, "Position estimation via ultra-wide-band signals," *Proc. IEEE*, vol. 97, no. 2, pp. 386–403, Feb. 2009.

[11] J. Rantakokko *et al.*, "Accurate and reliable soldier and first responder indoor positioning: Multisensor systems and cooperative localization," *IEEE Wireless Commun.*, vol. 18, no. 2, pp. 10–18, Apr. 2011.

[12] X. Shen and P. K. Varshney, "Sensor selection based on generalized information gain for target tracking in large sensor networks," *IEEE Trans. Signal Process.*, vol. 62, no. 2, pp. 363–375, Jan. 2014.

[13] J. J. Caffery, Jr., *Wireless Location in CDMA Cellular Radio Systems*. New York, NY, USA: Springer Science & Business Media, 2000.

[14] T. Zhang, Q. Zhang, H. Xu, H. Zhang, and B. Zhou, "Research and implementation of a practical ranging method using IR-UWB signals," *IEICE Trans. Commun.*, vol. E96-B, pp. 1976–1985, Jul. 2013.

[15] D. Dardari, A. Conti, J. Lien, and M. Z. Win, "The effect of cooperation on localization systems using UWB experimental data," *EURASIP J. Appl. Signal Process.*, vol. 2008, Feb. 2008, Art. no. 513873.

[16] H. Wymeersch, J. Lien, and M. Z. Win, "Cooperative localization in wireless networks," *Proc. IEEE*, vol. 97, no. 2, pp. 427–450, Feb. 2009.

[17] S. Li, M. Hedley, and I. B. Collings, "New efficient indoor cooperative localization algorithm with empirical ranging error model," *IEEE J. Sel. Areas Commun.*, vol. 33, no. 7, pp. 1407–1417, Jul. 2015.

[18] W. Dai, Y. Shen, and M. Z. Win, "Energy-efficient network navigation algorithms," *IEEE J. Sel. Areas Commun.*, vol. 33, no. 7, pp. 1418–1430, Jul. 2015.

[19] Y. Qi, H. Kobayashi, and H. Suda, "Analysis of wireless geolocation in a non-line-of-sight environment," *IEEE Trans. Wireless Commun.*, vol. 5, no. 3, pp. 672–681, Mar. 2006.

[20] Y. Shen, H. Wymeersch, and M. Z. Win, "Fundamental limits of wideband localization—Part II: Cooperative networks," *IEEE Trans. Inf. Theory*, vol. 56, no. 10, pp. 4981–5000, Oct. 2010.

[21] P. Chavali and A. Nehorai, "Scheduling and power allocation in a cognitive radar network for multiple-target tracking," *IEEE Trans. Signal Process.*, vol. 60, no. 2, pp. 715–729, Feb. 2012.

[22] W. W.-L. Li, Y. Shen, Y. J. Zhang, and M. Z. Win, "Robust power allocation for energy-efficient location-aware networks," *IEEE/ACM Trans. Netw.*, vol. 21, no. 6, pp. 1918–1930, Dec. 2013.

[23] H. Godrich, A. P. Petropulu, and H. V. Poor, "Power allocation strategies for target localization in distributed multiple-radar architectures," *IEEE Trans. Signal Process.*, vol. 59, no. 7, pp. 3226–3240, Jul. 2011.

[24] W. Dai, Y. Shen, and M. Z. Win, "Distributed power allocation for cooperative wireless network localization," *IEEE J. Sel. Areas Commun.*, vol. 33, no. 1, pp. 28–40, Jan. 2015.

[25] T. Wang, G. Leus, and L. Huang, "Ranging energy optimization for robust sensor positioning based on semidefinite programming," *IEEE Trans. Signal Process.*, vol. 57, no. 12, pp. 4777–4787, Dec. 2009.

[26] R. M. Vaghefi, M. R. Gholami, R. M. Buehrer, and E. G. Ström, "Cooperative received signal strength-based sensor localization with unknown transmit powers," *IEEE Trans. Signal Process.*, vol. 61, no. 6, pp. 1389–1403, Mar. 2013.

[27] N. Garcia, A. M. Haimovich, M. Coulon, and M. Lops, "Resource allocation in MIMO radar with multiple targets for non-coherent localization," *IEEE Trans. Signal Process.*, vol. 62, no. 10, pp. 2656–2666, May 2014.

[28] R. Rashtchi, R. H. Gohary, and H. Yanikomeroglu, "Joint routing, scheduling and power allocation in OFDMA wireless ad hoc networks," in *Proc. Int. Conf. Commun.*, Ottawa, ON, Canada, Jun. 2012, pp. 5483–5487.

[29] Y. Shen and M. Z. Win, "Fundamental limits of wideband localization—Part I: A general framework," *IEEE Trans. Inf. Theory*, vol. 56, no. 10, pp. 4956–4980, Oct. 2010.

[30] H. Godrich, A. M. Haimovich, and R. S. Blum, "Target localization accuracy gain in MIMO radar-based systems," *IEEE Trans. Inf. Theory*, vol. 56, no. 6, pp. 2783–2803, Jun. 2010.

[31] T. Zhang, C. Qin, A. F. Molisch, and Q. Zhang, "Joint power and spectrum allocation in wireless localization networks," *IEEE Trans. Commun.*, doi: 10.1109/TCOMM.2016.2580149.

[32] K. Haneda, A. Richter, and A. F. Molisch, "Modeling the frequency dependence of ultra-wideband spatio-temporal indoor radio channels," *IEEE Trans. Antennas Propag.*, vol. 60, no. 6, pp. 2940–2950, Jun. 2012.

[33] N. Michelusi, U. Mitra, A. F. Molisch, and M. Zorzi, "UWB sparse/diffuse channels, part I: Channel models and Bayesian estimators," *IEEE Trans. Signal Process.*, vol. 60, no. 10, pp. 5307–5319, Oct. 2012.

[34] Y. Shen, W. Dai, and M. Z. Win, "Power optimization for network localization," *IEEE/ACM Trans. Netw.*, vol. 22, no. 4, pp. 1337–1350, Aug. 2014.

[35] S. Dwivedi, A. De Angelis, and P. Händel, "Scheduled UWB pulse transmissions for cooperative localization," in *Proc. Int. Conf. Ultra-Wideband*, Syracuse, NY, USA, Sep. 2012, pp. 6–10.

[36] L. Song, T. Zhang, X. Yu, C. Qin, and Q. Zhang, "Scheduling in cooperative UWB localization networks using round trip measurements," *IEEE Commun. Lett.*, vol. 20, no. 7, doi: 10.1109/LCOMM.2016.2558499.

[37] S. Boyd and L. Vandenberghe, *Convex Optimization*. Cambridge, U.K.: Cambridge Univ. Press, 2004.

[38] D. C. Sorensen, "Newton's method with a model trust region modification," *SIAM J. Numer. Anal.*, vol. 19, pp. 409–426, Feb. 1982.

[39] N. M. Alexandrov, J. E. Dennis, Jr., R. M. Lewis, and V. Torczon, "A trust-region framework for managing the use of approximation models in optimization," *Struct. Optim.*, vol. 15, pp. 16–23, Feb. 1998.

[40] Y.-X. Yuan, "A review of trust region algorithms for optimization," in *Proc. Int. Congr. Ind. Appl. Math. (ICIAM)*, vol. 99. 2000, pp. 271–282.

[41] S. Boyd, *Sequential Convex Programming*. Stanford, CA, USA: Stanford Univ. Press, 2008.

[42] A. F. Molisch *et al.*, *IEEE 802.15.4a Channel Model—Final Report*, IEEE Standard P802-15-04, pp. 1–41, 2004.

[43] D. Dardari, A. Conti, U. Ferner, A. Giorgetti, and M. Z. Win, "Ranging with ultrawide bandwidth signals in multipath environments," *Proc. IEEE*, vol. 97, no. 2, pp. 404–426, Feb. 2009.

[44] V. Kristem, A. F. Molisch, S. Niranjayan, and S. Sangodoyin, "Coherent UWB ranging in the presence of multiuser interference," *IEEE Trans. Wireless Commun.*, vol. 13, no. 8, pp. 4424–4439, Aug. 2014.

[45] A. F. Molisch, *Wireless Communications*. New York, NY, USA: Wiley, 2010.

**Tingting Zhang** (M'12) received the B.S. (Hons.) and Ph.D. degrees in electronics engineering from the Harbin Institute of Technology (HIT), Harbin, China, in 2003 and 2009, respectively. From 2009 to 2012, he was a Post-Doctoral Research Fellow with the Communication Engineering Research Center, Shenzhen Graduate School, HIT, Shenzhen, China. From 2012 to 2014, he was with the Department of Electronic Engineering, University of Southern California, Los Angeles, CA, USA, as a Visiting Scholar. He is currently an Associate Professor with the Shenzhen Graduate School, HIT. His main research interests include cooperative localization, ultrawideband technology, and resource allocation. He serves as a TPC Member for several international conferences, such as GLOBECOM, ICCC, and VTC. He is also a Reviewer of numerous academic journals, such as the IEEE JOURNAL ON SELECTED AREAS IN COMMUNICATIONS, the IEEE TRANSACTIONS ON WIRELESS COMMUNICATIONS, and the IEEE TRANSACTIONS ON VEHICULAR TECHNOLOGY. He received the Outstanding Postdoctoral Award of HIT, Shenzhen Graduate School, in 2011. He also received the Shenzhen High Level Talent Program Award in 2012.

**Andreas F. Molisch** (S'89–M'95–SM'00–F'05) received the Dipl.-Ing., Ph.D., and Habilitation degrees from the Technical University of Vienna, Vienna, Austria, in 1990, 1994, and 1999, respectively. He subsequently was with AT&T (Bell) Laboratories Research (USA), Lund University, Lund, Sweden, and Mitsubishi Electric Research Labs (USA). He is currently a Professor of Electrical Engineering and the Director of the Communication Sciences Institute with the University of Southern California, Los Angeles. His current research interests are the measurement and modeling of mobile radio channels, ultrawideband communications and localization, cooperative communications, multiple-input multiple-output systems, wireless systems for healthcare, and novel cellular architectures. He has authored, co-authored, or edited four books [among them the textbook entitled *Wireless Communications* (Wiley-IEEE Press)], 18 book chapters, some 180 journal papers, 260 conference papers, and more than 80 patents and 70 standards contributions. Dr. Molisch has been an Editor of a number of journals and special issues, a General Chair, a Technical Program Committee Chair, or a Symposium Chair of multiple international conferences, and the Chairman of various international standardization groups. He is a Fellow of the National Academy of Inventors, AAAS, and IET, an IEEE Distinguished Lecturer, and a Member of the Austrian Academy of Sciences. He has received numerous awards, among them the Donald Fink Prize of the IEEE, and the Eric Sumner Award of the IEEE.

**Yuan Shen** (S'05–M'14) received the Ph.D. degree and the S.M. degree in electrical engineering and computer science from the Massachusetts Institute of Technology (MIT), Cambridge, MA, USA, in 2014 and 2008, respectively, and the B.E. degree (with highest honor) in electronic engineering from Tsinghua University, Beijing, China, in 2005.

He is an Associate Professor with the Department of Electronic Engineering at Tsinghua University. Prior to joining Tsinghua University, he was a Research Assistant and then Postdoctoral Associate with the Laboratory for Information and Decision Systems (LIDS) at MIT in 2005-2014. His research interests include statistical inference, network science, communication theory, information theory, and optimization. His current research focuses on network localization and navigation, inference techniques, resource allocation, and intrinsic wireless secrecy.

Dr. Shen was a recipient of the Qiu Shi Outstanding Young Scholar Award (2015), the China's Youth 1000-Talent Program (2014), the Marconi Society Paul Baran Young Scholar Award (2010), the MIT EECS Ernst A. Guillemin Best S. M. Thesis Award (1st place) (2008), the Qualcomm Roberto Padovani Scholarship (2008), and the MIT Walter A. Rosenblith Presidential Fellowship (2005). His papers received the IEEE Communications Society Fred W. Ellersick Prize (2012) and three Best Paper Awards from the IEEE Globecom (2011), the IEEE ICUWB (2011), and the IEEE WCNC (2007). He is elected Secretary (2015-2017) for the Radio Communications Committee of the IEEE Communications Society. He serves as symposium Co-Chair of the Technical Program Committee (TPC) for the IEEE Globecom (2016), the European Signal Processing Conference (EUSIPCO) (2016), and the IEEE ICC Advanced Network Localization and Navigation (ANLN) Workshop (2016). He also serves as Editor for the IEEE COMMUNICATIONS LETTERS since 2015 and Guest-Editor for the *International Journal of Distributed Sensor Networks* (2015).

**Qinyu Zhang** (M'08–SM'12) received the bachelor's degree in communication engineering from the Harbin Institute of Technology (HIT) in 1994, and the Ph.D. degree in biomedical and electrical engineering from the University of Tokushima, Japan, in 2003. From 1999 to 2003, he was an Assistant Professor with the University of Tokushima. From 2003 to 2005, he was an Associate Professor with the Shenzhen Graduate School, HIT, and the Founding Director of the Communication Engineering Research Center with the School of Electronic and Information Engineering. Since 2005, he has been a Full Professor, and serves as the Dean of the EIE School. His research interests include aerospace communications and networks, wireless communications and networks, cognitive radios, signal processing,and biomedical engineering.

He is on the Editorial Board of some academic journals, such as the *Journal on Communications*, *KSII Transactions on Internet and Information Systems*, and *Science China: Information Sciences*. He was the TPC Co-Chair of the IEEE/CIC ICCC'15, the Symposium Co-Chair of the IEEE VTC'16 Spring, an Associate Chair for Finance of ICMMT'12, and the Symposium Co-Chair of CHINACOM'11. He has been a TPC Member for INFOCOM, ICC, GLOBECOM, WCNC, and other flagship conferences in communications. He was the Founding Chair of the IEEE Communications Society Shenzhen Chapter.

He has received the National Science Fund for Distinguished Young Scholars, the Young and Middle-Aged Leading Scientist of China, and the Chinese New Century Excellent Talents in University, and obtained three scientific and technological awards from governments.

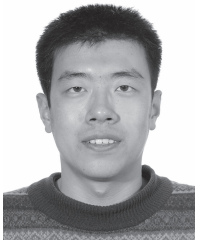

**Hao Feng** received the B.S. degree from the Department of Information Science and Electronic Engineering (ISEE), Zhejiang University, Hangzhou, China, in 2006, and the M.S. degree from the Wireless Communication Laboratory, ISEE, Zhejiang University, in 2008. He is currently pursuing the Ph.D. degree with the Department of Electrical Engineering, University of Southern California, Los Angeles, CA, USA. He has been with the Wireless Devices and Systems Group. He is a recipient of the Annenberg Graduate Fellowship for his Ph.D. study. His research interests include stochastic network optimization, cross-layer optimization, and cooperative communications with their applications in cloud networks, wireless ad-hoc networks, and wireless localization networks.

**Moe Z. Win** (S'85–M'87–SM'97–F'04) received both the Ph.D. in Electrical Engineering and the M.S. in Applied Mathematics as a Presidential Fellow at the University of Southern California (USC) in 1998. He received the M.S. in Electrical Engineering from USC in 1989 and the B.S. (*magna cum laude*) in Electrical Engineering from Texas A&M University in 1987.

He is a Professor at the Massachusetts Institute of Technology (MIT) and the founding director of the Wireless Information and Network Sciences Laboratory. Prior to joining MIT, he was with AT&T Research Laboratories for five years and with the Jet Propulsion Laboratory for seven years. His research encompasses fundamental theories, algorithm design, and experimentation for a broad range of real-world problems. His current research topics include network localization and navigation, network interference exploitation, intrinsic wireless secrecy, adaptive diversity techniques, and ultra-wideband systems.

Professor Win is an elected Fellow of the AAAS, the IEEE, and the IET, and was an IEEE Distinguished Lecturer. He was honored with two IEEE Technical Field Awards: the IEEE Kiyo Tomiyasu Award (2011) and the IEEE Eric E. Sumner Award (2006, jointly with R. A. Scholtz). Together with students and colleagues, his papers have received numerous awards, including the IEEE Communications Society's Stephen O. Rice Prize, (2012) the IEEE Aerospace and Electronic Systems Society's M. Barry Carlton Award (2011), the IEEE Communications Society's Guglielmo Marconi Prize Paper Award (2008), and the IEEE Antennas and Propagation Society's Sergei A. Schelkunoff Transactions Prize Paper Award (2003).

Dr. Win was an elected Member-at-Large on the IEEE Communications Society Board of Governors (2011-2013). He was the Chair (2004-2006) and Secretary (2002-2004) for the Radio Communications Committee of the IEEE Communications Society. Over the last decade, he has organized and chaired numerous international conferences.